Tag Position Estimation in RFID Systems

by

Yi Li

B.E. (Electrical & Electronic),
University of Electronic Science and Technology of China

Thesis submitted for the degree of

Master of Philosophy

in

School of Electrical and Electronic Engineering
The University of Adelaide, Australia

Dec 2012

THE UNIVERSITY
OF ADELAIDE
AUSTRALIA

Typeset in LaTeX 2ε

Yi Li

To my parents

Contents

Abstract

In order to find people, locate intruders and navigate patients along a building, various wireless positioning technologies have been researched. Compared with the other wireless positioning techniques, RFID has some obvious advantages of low cost, long lifespan and energy efficiency. All these advantages make RFID a good choice to implement wireless positioning systems in an indoor environment.

Radio frequency identification (RFID) is a technology that utilizes electromagnetic waves to convey information between an RFID reader (also called as an interrogator) and an RFID tag in order to identify and track the object to which the tag is attached. According to the power sources of RFID tags, RFID systems can be divided into two types: active RFID and passive RFID. While active RFID systems are better for outdoor localization, passive RFID systems are more suitable for indoor positioning. For the special modulation scheme 'backscattering' of passive RFID systems, we can estimate the position of tags according to the phase differences between the transmitted signal and the backscattered signal (PDOA).

In this thesis, we have proposed a structure that can be used to measure the phase differences between the transmitted signals and the backscattered signals. After proposing the structure, it is analyzed mathmatically. Some simulations with the software Simulink are also performed to theoretically verify the effectiveness of the proposed structure.

According to the proposed structure, we set up a hardware platform. Using the hardware, several tests were made and based on the analysis of the test results, the effectiveness and efficiency of the proposed structure has been verified practically.

Statement of Originality

This work contains no material that has been accepted for the award of any other degree or diploma in any university or other tertiary institution and, to the best of my knowledge and belief, contains no material previously published or written by another person, except where due reference has been made in the text.

I give consent to this copy of the thesis, when deposited in the University Library, being available for loan, photocopying and dissemination through the library digital thesis collection.

The author of this thesis acknowledges that copyright of published work contained within this thesis (as listed in the publications page) resides with the copyright holder(s) of that work.

Signed

Date

Acknowledgments

First and foremost, I must recognize my principal supervisor Dr. Behnam Jamali for his constant and patient guidance during the period of my master study. His meticulous approach to learning and tolerance towards others will influence me for the rest of my life. Talking with him not only in professional areas but also on other topics such as culture has always been enjoyable and beneficial.

I would also like to wholeheartedly thank my co-supervisors Mr. Matthew Trinkle for providing valuable suggestions to my research.

Sincere thanks also to my colleagues in the School of Electrical and Electronic Engineering for their unselfish help in extending my knowledge. They are Mark Jessop, Geng Tian and Ruiting Yang.

I am indebted for the work done by the staff in the School of Electrical and Electronic Engineering, particularly, Associate Professor Cheng-Chew Lim and Mr Stephen Guest. Of course thanks to the four kind ladies in the school office.

Many thanks to my friends, specifically Zhonghao Hu, Yuexian Wang, and Liang Duanmu in Adelaide for their constant support and encouragement during my master studies.

I am grateful to my parents who dedicate their unconditional love and encouragement to me. Since I first entered primary school, all through my educational journey of twenty years, their love has always accompanied me. Without them, I could not imagine how I could have accomplished this work.

Yi Li (May 2012)

Conventions

Typesetting

This thesis is typeset using the LaTeX2e software.

The fonts used in this thesis are Times New Roman and Sans Serif.

Referencing

Referencing and citation style in this thesis are based on the Institute of Electrical and Electronics Engineers (IEEE) Transaction style [1].

For electronic references, the last accessed date is shown at the end of a reference.

Units

The units used in this thesis are based on the International System of Units (SI units) [2].

Spelling

The Australian English spelling is adopted in this thesis.

Abbreviations

ASK Amplitude Shift Keying

CW Continuous Wave

FD-PDOA Frequency Domain PDOA

GPS Global Positioning System

IEC International Electrotechnical Commission

ISO International Organization for Standardization

PDOA Phase Difference Of Arrival

PSK Phase Shift Keying

RF Radio Frequency

RFID Radio Frequency Identification

RSSI Received Signal Strength Indication

SD-PDOA Spatial Domain PDOA

TDOA Time Difference Of Arrival

TD-PDOA Time Domain PDOA

UWB Ultra-WideBand

WLAN Wireless Local Area Network

List of Figures

Chapter 1

Introduction and Motivation

THIS chapter gives a brief introduction to the positioning technology in RFID systems. The research problems and the contributions of this thesis are presented. Finally, the thesis structure is discussed and the contents of each chapter are summarized.

1.1 Research Area

1.1.1 Introduction of RFID

Radio frequency identification (RFID) is a technology that utilizes electromagnetic waves to convey information between an RFID reader (also called as an interrogator) and an RFID tag in order to identify and track the object to which the tag is attached [3]. Unlike the traditional bar-code labeling technique, RFID enables identification from a distance [4]. As is shown in Fig. 1.1, a typical RFID system is composed of three parts: a reader, a tag and antennas on the tag and on the reader that are used to mediate between voltages and currents on wires and radio waves in the air. With the unprecedented increase in capability and decrease in cost of electronics, the advantage of RFID for object tracking and inventory management has become increasingly significant. Consequently, RFID has been increasingly widely used in many industries, including supply chain management [5], remote health care [6], retail industry [7], hospitality [8], food industry [9] [10] and airline industry [11]. To regulate the RFID industry, some standards have been set by various organizations like the International Organization for Standardization (ISO), the International Electrotechnical Commission (IEC), ASTM International, the DASH7 Alliance and EPCglobal [12]. Based on the RFID and some other techniques like bar-codes and 2D-codes, the Internet of Things has been developing with unprecedent pace to allow objects used in daily life to be identified and inventoried by computers [13].

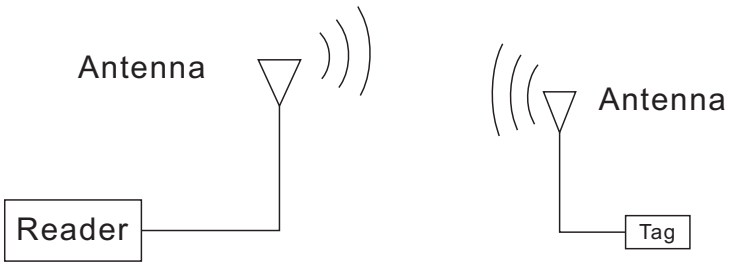

Figure 1.1. Basic Structure of RFID Systems

1.1.2 Introduction to wireless positioning technology

In order to localize or track an object, a lot of wireless positioning technologies have been utilized. The earliest application was to use acoustic waves to localize underwater submarines for military use [14]. The utilization of radar to position flying aircraft played an important role in World War II [15]. After World War II, the most famous application of wireless localization is the Global Positioning System (GPS) developed by U.S. Department of Defense (USDOD). A GPS receiver uses time of arrival of signals from different satellites to calculate its position. The use of wireless local area network (WLAN) equipment to position objects based on the Received Signal Strength Indication (RSSI) has also been developed recently [16]. Infrared waves have also been used to estimate the position of some objects like mobile robots [17] while the ultrasonic waves have been used in the applications involving human interface [18].

1.1.3 Introduction of object positioning in RFID system

In order to find people, locate intruders and navigate patients along a building, various technologies have been adopted. Some of these technologies are infrared, LAN and ultrasonic. Compared to these localization techniques, RFID has some inherent advantages. The features of contactless communications, high data rate and security, non line-of-sight readability, compactness and low cost have made RFID a good candidate to position objects in an indoor environment [19].

There are several parameters that can be used to estimate position in RFID systems: TDOA [20], RSSI [21] and PDOA (Phase Differences of Arrival) [22]. Due to the limited read range in RFID systems, the time difference of arrival at different receiver antennas would be too small (less than 1 nanosecond) to be measured with simple interrogators. The RSSI based method is not a good choice either because the propagation environment will substantially affect the measurement correctness of RSSI [23]. Moreover, the absolute calibration needed for RSSI measurements is rather difficult [23]. Consequently, the PDOA based method is the most attractive way to estimate position in RFID systems.

1.2 Research Problems

PDOA can be used in three main ways to determine the position of RFID tags: Time domain (TD-PDOA), frequency domain (FD-PDOA) and spatial domain (SD-PDOA). While these techniques have been proposed in the literature [23], most paper do not describe how to obtain the PDOA information from an RFID system. Without an effective and efficient way to obtain the PDOA information, all the three mentioned applications TD-PDOA, FD-PDOA and SD-PDOA cannot be used. Moreover, most papers do not explain how to implement such a positioning system based on PDOA measurements. Therefore, a specific hardware platform is needed to demonstrate how to implement a tag positioning systems using PDOA information.

1.3 Original Contributions

In order to solve the research problems mentioned in the Section 1.2, we have completed a research project implementing PDOA based tag positioning. Our research contributions in this thesis are summarized as follows:

- A reader structure that can be used to obtain PDOA values is proposed. Based on this structure, three systems based on TD-PDOA, FD-PDOA and SD-PDOA measurements can be implemented to estimate the position of tags in an indoor environment.

- A simulation with the software Simulink has been run to theoretically verify the validity of the proposed structure.

- Two hardware platforms have been made according to the proposed structure in this thesis. After completing the hardware, some tests have been performed and the measured data was analyzed. Thus the effectiveness of the proposed structure is verified practically.

1.4 Thesis Structure

The thesis is presented in five chapters:

Chapter 1 provides a brief introduction to PDOA based tag positioning. In this chapter, RFID technology and various wireless localization techniques are introduced separately. In addition, the research problems and original academic contributions are also defined.

Chapter 2 presents the background including the various techniques used for the wireless positioning, the different parameters that can be used to get the positioning information and three specific applications of PDOA based positioning in RFID systems (TD-PDOA, FD-PDOA and SD-PDOA).

Chapter 3 introduces the main theoretical work in this research project. The structure that can be used to get PDOA information is proposed in this chapter. In addition, a software simulation has been performed to theoretically verify the validity of this proposed structure.

Chapter 4 describes the implementation of a hardware platform according to the proposed structure. Based on this hardware platform, some tests are preformed and the test results are analyzed to verify the validity of the PDOA based positioning methodology. The hardware platform used in this section is based on a commercially available system which could be used directly with minor modifications.

Chapter 5 introduces the implementation of our own hardware platform, also based on the proposed structure, which can also be extended to a multi-antenna RFID system. The PDOA technique is also tested on this hardware platform.

Chapter 6 reviews and concludes the thesis. In addition, some recommendations for future work are given. Finally, the original contributions to knowledge are re-summarized.

Chapter 2

Background

THIS chapter contains details of various techniques for wireless positioning. The comparison of different indoor positioning techniques provides a clear indication that RFID is a good choice to implement a positioning systems in an indoor environment. The three applications of PDOA are also illustrated in this chapter.

2.1 Introduction

Due to the increasing requirement of ubiquitous computing and the fast development of Internet of Things, wireless positioning or localization technologies have been gaining great interest in the wireless area. In the field of wireless positioning, many techniques have already been widely utilized worldwide. The Global Positioning System (GPS), Sonar and laser scanning are the main three outdoor localization techniques. Besides these three techniques, infrared, wireless local area network (WLAN), RFID, and ultrasonic wave can also be used for positioning objects. This chapter firstly introduces the three localization technologies-GPS, sonar systems, laser scanning and explain why they are not suitable for the indoor environment. Then a simple comparison of the indoor wireless positioning techniques is made. After that, some classifications of indoor positioning system with RFID technology from different points of view are illustrated. In the end, the three specific applications of PDOA based techniques-TD-PDOA, FD-PDOA and SD-PDOA are introduced for RFID positioning.

2.2 Outdoor Wireless Localization Techniques

GPS, sonar systems and laser scanning are three outdoor wireless localization techniques. However, all the three techniques are not suitable for the indoor environment. In this section, the reasons why they are not suitable for the indoor environment are analyzed separately.

2.2.1 GPS

The Global Positioning System (GPS) [24] is a satellite based localization system that can provide both the position and time information. In order to get enough information for the calculation of an object's position and time, signals from at least 4 satellites should be received and demodulated. The signals from every satellite convey the information of the satellite's position and the time when the signals is transmitted. The GPS receiver uses the Time Of Arrival (TOA) information from several satellites to calculate its own location information and time. With 24 satellites since 1994, the whole

earth can be covered and one can get enough information from at least four satellites anywhere on the earth.

However, the GPS system has some unescapable disadvantages that make it not suitable for indoor applications. Firstly, the GPS signal from the satellites is so weak that it cannot go through a wall to be received by indoor equipment [25]. Moreover, it cannot provide enough accuracy for the indoor positioning. Although some advanced GPS receivers using differential corrections from systems such as the Nationwide Differential GPS can achieve an accuracy of $1 - 2$m which is much better than the traditional GPS systems [26] [27], it is still too inaccurate for indoor applications.

In summary, while GPS has many advantages for outdoor localization, it is not a good choice for indoor position estimation. However, GPS could potentially be used together with another indoor localization technology to track objects moving between indoor and outdoor environments [28]. We can also utilize GPS signal repeaters to make the GPS signal available in an indoor environments [29].

2.2.2 Sonar Systems

Sonar systems are widely used for the localization of objects in underwater environments. Like GPS, Sonar systems were also developed initially for military use. Sonar systems don't use electromagnetic wave as in GPS but acoustic waves to estimate an underwater object's position. A typical sonar system uses a sensor array to receive the backscattered acoustic wave from the object [30]. Based on the time differences of arrival of the acoustic wave, the sonar system can calculate the position of the object. Thus sonar systems locate the object from the same TOA information as GPS.

Sonar systems behave well because the acoustic waves are attenuated much less in water than the electromagnetic waves. While in the air, the acoustic waves are attenuated much more than electromagnetic. Therefore, Sonar systems are not applicable in an indoor environment either.

2.2.3 Laser Scanning

Besides GPS and Sonar systems, there is another outdoor localization technique called laser scanning. This technique is mostly used on vehicles to avoid collisions through the localization information of the surrounding objects [31]. However, this technique is not suitable for the indoor application because it requires line-of-sight imaging which is usually not applicable in indoor environment.

2.3 Comparison of Different Indoor Positioning Techniques

Due to its low cost and no requirement for an embedded battery, RFID is more promising for indoor positioning than other indoor localization techniques such as WIFI, wireless sensor networks, ultrasound, infrared and video cameras is the low cost. An RFID tag can cost much less than general-purpose wireless sensor nodes [32].

Hui Liu et al. [33] made a survey of wireless indoor positioning techniques in 2007. In their paper, they analyzed the advantages and disadvantages of several wireless techniques including GPS, RFID, cellular, UWB, WLAN and Bluetooth. They examined a set of properties by which positioning techniques are evaluated. These wireless techniques are compared with each other in terms of accuracy, precision, complexity, scalability, robustness, and cost. According to their conclusion, RFID technology has advantages in terms of cost but is not competitive in terms of precision.

In their technical report "A Survey and Taxonomy of Location Systems for Ubiquitous Computing" [34], J. Hightower and G. Borriello listed three techniques other than RFID used to estimate position in an indoor environment: infrared, WLAN and ultrasonic. They also discussed the drawbacks of these three technologies respectively. Infrared localization is considered in that report as not suitable for indoor location sensing due to its very short-range signal transmission. A positioning system based on WLAN equipment utilizes RSSI and signal-noise ratio (SNR) to sense the location of object. The required WLAN equipment will be relatively large and consume a lot of energy. The localization method using ultrasonic sensor networks is not a good solution because it requires significant infrastructure to accurately determine the location. K. Yamano [19]

believed RFID is the best choice to estimate position in indoor environment because of its features of contactless communications, security, non line-of-sight readability, compactness and low cost.

2.4 Classifications of Indoor Positioning System with RFID Technology

RFID based positioning system can be classified in different ways. Based on whether the tag is powered or not, RFID positioning technology can be classified into two groups: active RFID based positioning systems and passive RFID based positioning systems. In terms of parameters used to estimate position, RFID based positioning systems can be classified into TDOA based, RSSI based and PDOA based systems.

2.4.1 Active and Passive

Passive RFID based positioning systems refer to those RFID positioning systems that use passive tags. As shown in the Fig. 2.1, a passive tag does not require batteries and gets its power supply from the electromagnetic wave transmitted from an RFID reader [35]. The passive tags don't need transmitters to transmit signals but use a process of backscattering instead [36]. This special modulation scheme of backscattering also means PDOA values can be used for position estimation in passive RFID systems. Without batteries and transmitters, passive tags can cost much less than active tags. Moreover, the sizes of passive tags are much smaller than active ones. Removing the need to change batteries, passive tags also have a much longer lifespan. With these three advantages, Passive RFID based positioning systems are more suitable than their active counterparts for indoor environments in most cases. This project focused on the Passive RFID based positioning systems.

Active RFID based positioning systems refer to those RFID positioning system that use active tags. Unlike the passive tags, active tags have their own power supply and transmitter, as is shown in the Fig. 2.2. Although active tags are not suitable for indoor

environments as mentioned above, they are good choices to implement positioning systems for outdoor application because they have much longer reader ranger than passive tags.

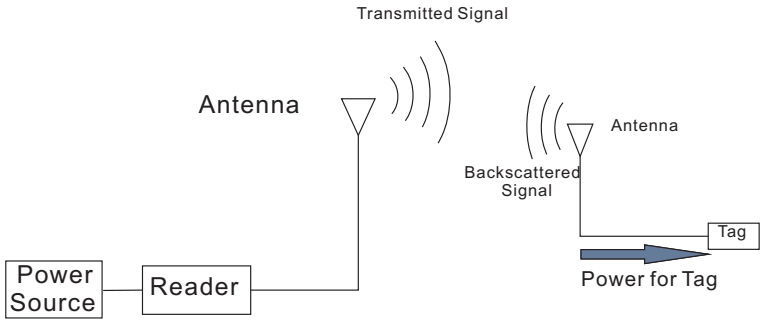

Figure 2.1. Passive RFID system

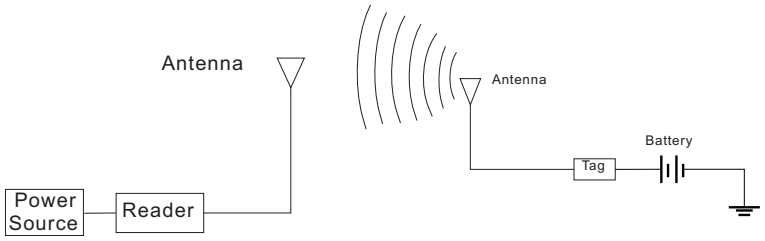

Figure 2.2. Active RFID system

2.4.2 TDOA, RSSI and PDOA

The time difference of arrival (TDOA) parameter is widely used in wireless positioning. The most famous application of this parameter is GPS. To use TDOA information to calculate position, the positioning equipment should be able to receive signals from various sources. According to the time differences of arrival of the various signals and the known position of the signal sources, the equipment can calculate its own position. In an indoor environment, the distance differences of the various signal sources to the receiver are barely longer than 10 meters.Therefore, the time differences of arrival will be smaller than $\frac{10}{3\times10^8} = 33.3ns$. It is difficult to measure such small time differences accurately, especially considering the limited signal bandwidth of most RFID systems of less than 1MHz [36], and a simple receiver structure. Thus TDOA is not considered in this thesis for RFID indoor positioning.

The received strength indication (RSSI) is also widely used for position estimation. A typical application of RSSI is that in cellular communication systems, the base station utilizes the RSSI value to estimate the distance between mobile phones and the base station. However, the performance of RSSI based wireless positioning is degraded significantly by the multipath effects in an indoor environment [23].

J. Zhou and J. Shi proved that some of the parameters used to estimate position like TDOA, RSSI and PDOA are also applicable to RFID [37]. In the paper "Phase Based Spatial Identification of UHF RFID Tags" [23], Pavel V. Nikitin et al. have compared these three different approaches and then concluded that the PDOA approach is much better to implement in an RFID positioning system than the other two ways in terms of measurement correctness, simplicity of structure, cost and energy consumption. They also mentioned that if PDOA is used, the propagation channel and the modulating properties on which phase of the tag signal depends can be calibrated.

2.5 Applications of PDOA Based RFID Positioning Systems

In [23], Pavel V. Nikitin et al. divided PDOA based positioning methods into three main categories: Time Domain (TD)-PDOA, Frequency Domain (FD)-PDOA and Spatial Domain (SD)-PDOA. Through the measurement of tag phases at different time points, TD-PDOA can be used to estimate the radial velocity of tags. FD-PDOA, on the other hand, enables one to calculate the distance to the tag by measuring the tag phase at different frequencies. This technique is similar to the TDOA based positioning introduced in the previous section, but it extends the bandwidth of the signal by measuring the phase at different carrier frequencies and thus obtaining a more accurate time delay measurement. SD-PDOA is a form of direction-of-arrival estimation using a phased array antenna. SD-PDOA can be utilized to estimate the angle of arrival through the measurement of phases of the tag signal at several receiving antennas.

The principles of these three applications of the PDOA based RFID positioning systems are illustrated in the following three sections. All the following formulae are based on

the assumption that the RFID system is working in a communication environment similar to free space. Based on this assumption, we can obtain the total time needed for a signal to be transmitted from an RFID reader to a tag and then backscattered to the reader:

$$t_{total} = t_{forward} + t_{reverse} \tag{2.1}$$

The $t_{forward}$ stands for the time needed for a signal to be transmitted from an RFID reader to a tag while $t_{reverse}$ means the time required for a signal to be backscattered to the reader. We denote the distance between the tag and the reader as d, so $t_{forward}$ and $t_{reverse}$ can be calculated as follows:

$$t_{forward} = t_{reverse} = \frac{d}{c} \tag{2.2}$$

From equation(2.1) and equation(2.2), the t_{total} can be obtained:

$$t_{total} = \frac{2d}{c} \tag{2.3}$$

The relation between phase φ and propagation time t is :

$$\varphi = \frac{-t}{T} * 2\pi = \frac{-t}{\frac{1}{f}} * 2\pi \tag{2.4}$$

Where T is the period of one oscillation and f is the frequency of oscillation of the RF carrier. Together with equation(2.3), we can obtain:

$$\varphi = \frac{-4\pi * d * f}{c} \tag{2.5}$$

2.5.1 TD-PDOA

As is seen in Figure 2.3, the velocity of a tag can be divided into two parts: V_r for the velocity component in the direction of the line of sight between the tag and the reader

while V_t is the velocity component perpendicular to the line of sight between the tag and the reader. The phase differences at different time points can be used to calculate the component of the velocity V_r.

$$V_r = \frac{\partial d}{\partial t} \tag{2.6}$$

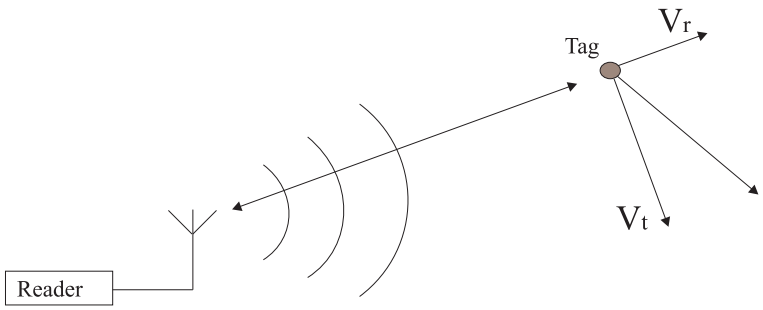

Figure 2.3. TD-PDOA

Together with equation(2.5), we can obtain:

$$V_r = \frac{c}{4\pi * f}\frac{\partial \varphi}{\partial t} \tag{2.7}$$

From the equation(2.7), we can perform the experiment of making the tag move at a fixed radial velocity, then measuring the PDOA at different time points. With the measured data and equation(2.7), we will check the consistency between calculated velocity and a fixed radial velocity. Thus the formula can be verified by the experiment.

2.5.2 FD-PDOA

From Figure 2.4, we can obtain a scheme for estimating the distance between a tag and a reader. The PDOA will be measured when RF signals of different frequencies are transmitted. From equation(2.5), we can obtain:

$$d = \frac{c}{4\pi}\frac{\partial \varphi}{\partial f} \tag{2.8}$$

The validity of the formula will be checked by making the RFID reader send signals at different frequencies and recording the phase of the returned signals.

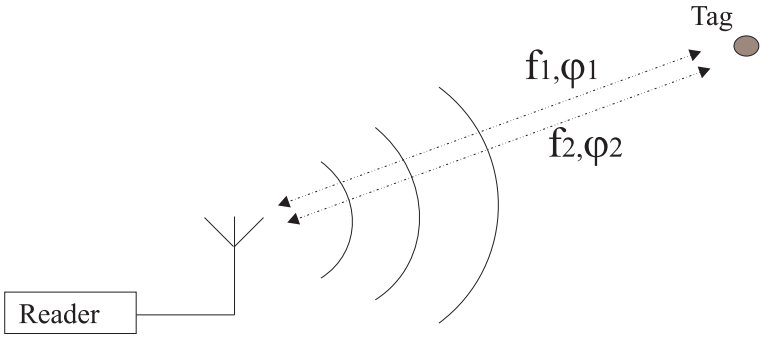

Figure 2.4. FD-PDOA

2.5.3 SD-PDOA

2.5.3.1 Two Receiver Antennas

As illustrated in Figure 2.5, when the tag is far enough from the two receiver antennas, the angle θ_1 is small enough to be ignored. Let $AB = AC$, so the angles θ_2 and θ_3 are the same value of $\frac{\pi}{2}$. The length of CD (d_0) will be AB-AD or $d_1 - d_2$, and can be calculated as:

$$d_0 = d_1 - d_2 = \frac{c}{2\pi}\frac{\varphi_1}{f} - \frac{c}{2\pi}\frac{\varphi_2}{f} \tag{2.9}$$

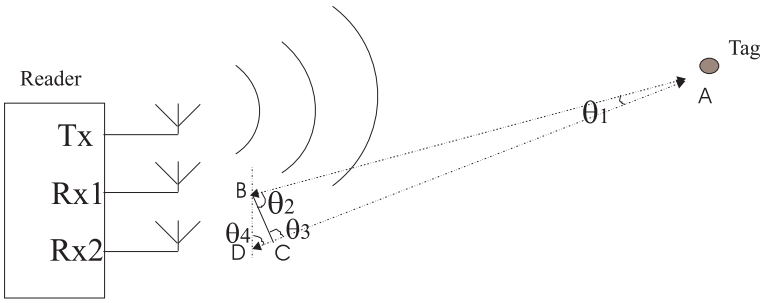

Figure 2.5. SD-PDOA

From the above equation, the angle of arrival θ_4 could be calculated:

$$\theta_4 = \arccos\frac{c}{2\pi * f}\frac{\varphi_1 - \varphi_2}{a} \tag{2.10}$$

Where a is the distance between the two receiver antennas (BD). It is also notable that if the AB-AD is longer than the one wavelength ($\lambda = \frac{c}{f}$), the above equation has ambiguities.

2.5.3.2 More Receiver Antennas

If there are more than two receiver antennas, there will be more than two equations to calculate the position of a tag even when the reader is close to the tag. In this case more generalized beamforming techniques could be applied to estimate the direction of arrival of the tag [38] [3] [39].

2.6 Conclusion

This chapter has introduced various techniques that can be used in wireless positioning. Among these techniques, RFID emerges as a competitive candidate for indoor wireless positioning applications because of its features of contactless communications, high data rate, security, non line-of-sight readability, compactness and low cost [19]. The RFID systems using passive tags outperform those using active ones in an indoor environment due to the smaller size of the tags, lower costs and longer lifespan. Among the three different parameters TDOA, RSSI and PDOA that can be used to estimate position, PDOA appears to be the best choice.

Beside introducing different techniques, this chapter also describes three different applications of PDOA based RFID positioning systems: TD-PDOA, FD-PDOA and SD-PDOA.

Chapter 3

Proposed Structure to obtain PDOA Measurements

THIS chapter proposes a structure that can be used to obtain PDOA measurements in passive RFID systems. In addition, a software tool Simulink is used to simulate this proposed structure and thereby verify its validity.

3.1 Introduction

In chapter 2, three specific applications of PDOA based positioning in RFID systems (TD-PDOA, FD-PDOA and SD-PDOA) have been introduced. It was also found that in an indoor environment, passive RFID systems using RFID tags have several advantages over the active systems. In addition, some advantages of the PDOA based positioning methodology were introduced by comparing it with methodologies based on RSSI and TDOA parameters. Therefore, this chapter focuses on PDOA based positioning in passive RFID systems.

This chapter includes four main parts. The first part proposes a structure that can be used to obtain the PDOA values in a passive RFID systems. In the second part a mathematical analysis of the structure is carried out to verify its validity. Two different modulation schemes-Amplitude Shift Keying (ASK) and Phase Shift Keying (PSK) have been considered in the analysis. In the third part, the potential problem of leakage signals from the transmission chain into the receiver chain has been analyzed. Finally, a simulation of the proposed structure with the software tool Simulink is introduced in the last part.

3.2 Relationship between Phase Difference and Distance in Passive RFID systems

According to the EPC global protocol [36], passive tags in RFID systems don't have their own source of energy to drive their circuitry. In order to send information to the RFID readers, the passive tags modify their interaction with the transmitted signals from the RFID readers at the same time rectifying the received power to support their operation. This is the process of backscattering.

Fig. 3.1 shows a simple structure of the backscatter modulation for passive RFID systems. In this figure, we can see that in the time frame when it is receiving, an RFID reader transmits a continuous wave (CW) signal while receiving the reflected signal from the tags. We denote the transmitted CW signal from RFID reader as $A_0 \cos(\omega t)$.

The ω stands for the angular frequency of the CW signal and A_0 is the amplitude. When the reflected signal arrives at the antenna of the RFID reader, it will be delayed relative to the transmitted signal $A_0\cos(\omega t)$. Therefore, we can denote the backscattered signal at the antenna as $A_1\cos(\omega t - \varphi)$. A_1 is the amplitude of the backscattered signal which is much smaller than that of the transmitted signal due to the path loss. The φ is the phase difference between the two signals due to the time delay between them and according to Equation(2.5), $\varphi = -\frac{-4\pi * d * f}{c}$.

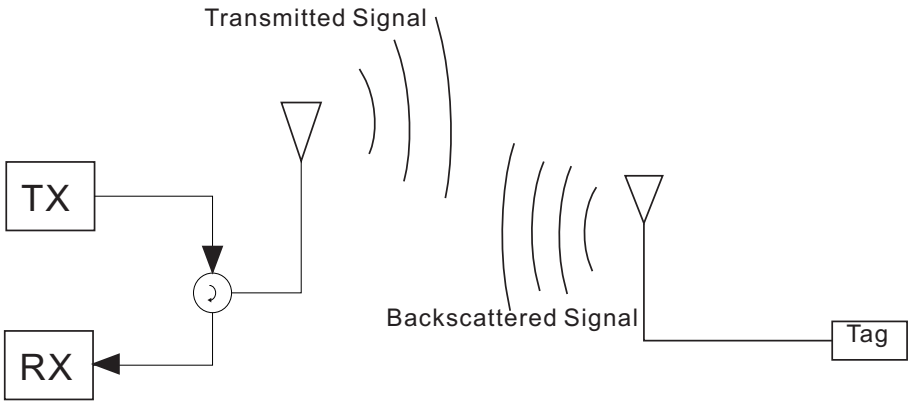

Figure 3.1. Scheme of backscattering

3.3 Proposed Structure

The simplified structure shown in the Fig. 3.2 can be used to obtain the phase difference between the transmitted and the backscattered signals.

From the diagram, we can see that the RFID reader will receive the backscattered signal while transmitting the LO (Local Oscillator) signal to the tag. Two mixers are used to multiply the received signal with the LO signal and a 90^o phase shifted version of the LO signal respectively. The two chains are named as In phase (I) chain and Quadrature (Q) chain. After mixing, the resulting signals should be:

$$I = A_0\cos(\omega t) \times A_1\cos(\omega t - \varphi) = \frac{1}{2}A_1A_0[\cos(2\omega t - \varphi) + \cos\varphi] \tag{3.1}$$

$$Q = A_0\sin(\omega t) \times A_1\cos(\omega t - \varphi) = \frac{1}{2}A_1A_0[\sin(2\omega t - \varphi) - \sin\varphi] \tag{3.2}$$

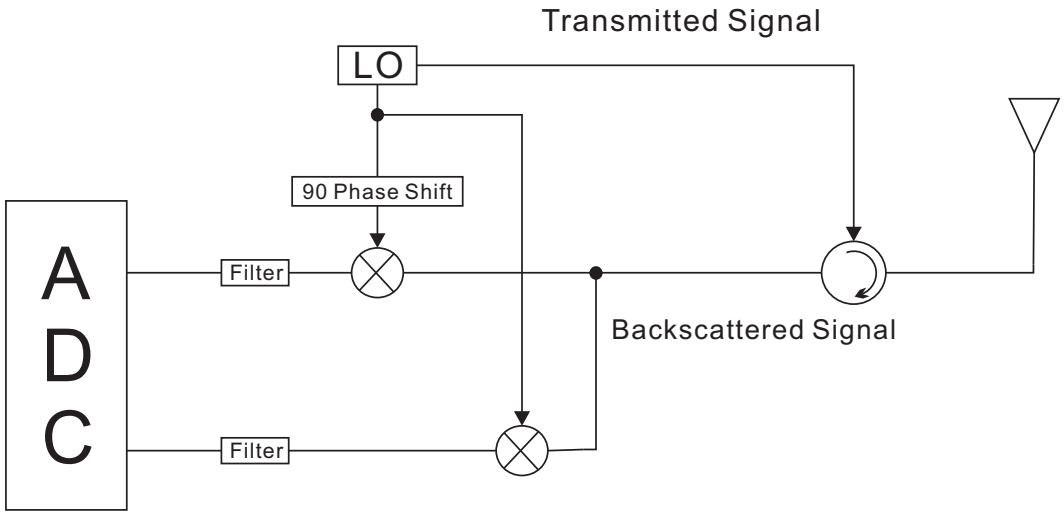

Figure 3.2. struture

After the Low Pass Filter (LPF), the remaining signals should be:

$$I = \frac{1}{2} A_0 A_1 \cos\varphi \qquad (AfterLPF) \tag{3.3}$$

$$Q = -\frac{1}{2} A_0 A_1 \sin\varphi \qquad (AfterLPF) \tag{3.4}$$

From Equation(3.12) and Equation(3.13), the phase difference φ between the transmitted signal and the backscattered signals can be calculated from the following formula:

$$\varphi = \arctan(-\frac{Q}{I}) + k\pi \qquad (k = 0, \pm 1, \pm 2 \cdot \cdot \cdot \cdot \cdot \cdot) \tag{3.5}$$

The differences in the above equation is ambiguous in k. However, as we mainly consider the differences in φ over a range of frequencies, the k factor will be canceled out in most situations considered.

3.4 ASK and PSK

There are two ways for the passive tags to modulate their bit information (1s and 0s) onto the backscattered signal: Amplitude Shift Keying (ASK) and Phase Shift Keying

(PSK). ASK modulates its bit stream on to the CW signal by changing the amplitude. PSK, on the other hand, changes the phase of CW signal according to the bit stream that the passive tag wants to send. Detail information comparing these two modulation schemes can be found in the book 'The RF in RFID: passive UHF RFID in practice' [40].

3.4.1 ASK

Fig.3.3 shows two different operating modes of RFID passive tags using the ASK scheme. The first one is called normal mode as in this mode, the antenna and the IC have been matched to maximise the power transfered into the IC. If we define the total voltage impinging on the antenna as V_{total}, the current going through the IC can be obtained as follows:

$$I_{normal} = \frac{V_{total}}{R_{antenna} + R_{ic}} \tag{3.6}$$

The $R_{antenna}$ and R_{ic} are the resistances of antenna and IC respectively. Therefore, the power delivered into the IC is:

$$P_{ic} = I_{normal}^2 \times R_{ic} \tag{3.7}$$

Together with the Equation (3.6), the power delivered into the IC P_{ic} can be obtained as:

$$P_{ic} = \frac{V_{total}^2}{(R_{antenna} + R_{ic})^2} \times R_{ic} \tag{3.8}$$

In order to get the largest powered delivered to the IC, R_{ic} should be equal to $R_{antenna}$, and the power delivered into the IC is:

$$P_{ic} = \frac{V_{total}^2}{4 \times R_{antenna}} \tag{3.9}$$

In this case, the power reflected from the antenna $P_{antenna}$ is the same as P_{ic} and the voltage of the backscattered signal is $\frac{V_{total}}{2}$.

The second mode of ASK is called short mode as there is a short circuit presented to the antenna. In the short mode, there is no current going through the IC and no power delivered to the IC. The IC uses stored energy in the tag to continue to function during this time. The current going through the antenna can be calculated as $\frac{V_{total}}{R_{antenna}}$ and the amplitude of the back scattered signal is V_{total} which is two times larger than in normal mode.

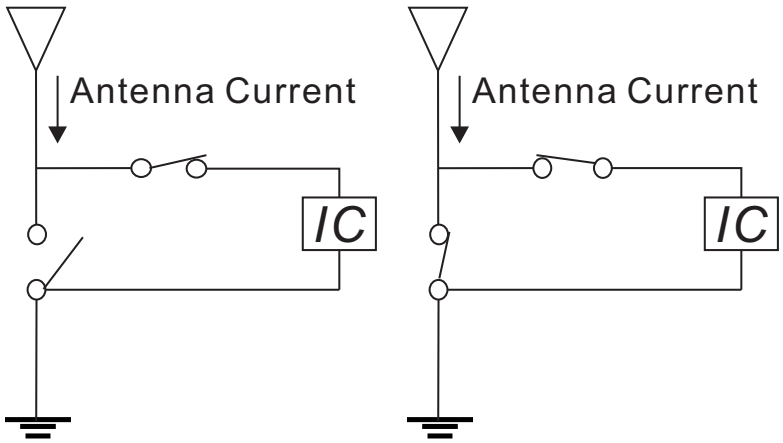

(a) Normal mode (b) Short mode

Figure 3.3. Two different operating modes of ASK

In summary, we conclude that the amplitude of the backscattered signal is half of the amplitude of the impinging signal in normal mode while in the short mode, the amplitude of the backscattered is the same as the impinging signal. Table 3.1 summarizes the comparison of the two operation modes.

Table 3.1. Comparison of ASK Modes

Modes	Amplitude of Backscattered Signal	Power delivered to IC
Normal Mode	$\frac{V_{total}}{2}$	$\frac{V_{total}^2}{4 \times R_{antenna}}$
short mode	V_{total}	0

In order to simplify the theoretical model used in this report, we assume that the tag uses the normal mode to convey a '1' and the short mode to convey a '0'. So the backscattered signal arriving at the antenna of the RFID reader can be denoted as: $C_1(t) * A_1 \cos(\omega t - \varphi)$. Where $C_1(t)$ is the rectangular wave as in the Fig. 3.4

In the case of ASK, the output signals of the two mixers would be:

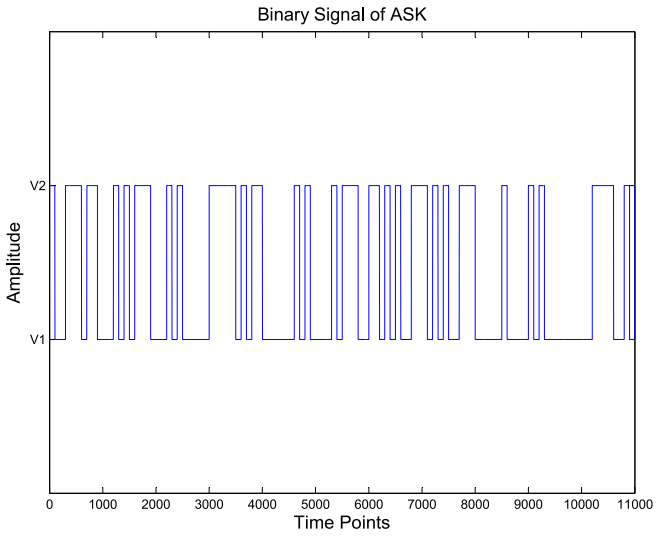

Figure 3.4. Binary signal of ASK

$$I = A_0 \cos(\omega t) \times C_1(t) * A_1 \cos(\omega t - \varphi) = \frac{1}{2} A_1 A_0 C_1(t)[\cos(2\omega t - \varphi) + \cos\varphi] \quad (3.10)$$

$$Q = A_0 \sin(\omega t) \times C_1(t) * A_1 \cos(\omega t - \varphi) = \frac{1}{2} A_1 A_0 C_1(t)[\sin(2\omega t - \varphi) - \sin\varphi] \quad (3.11)$$

After the LPF, the remaining signals would be:

$$I = \frac{1}{2} C_1(t) A_0 A_1 \cos\varphi \qquad (AfterLPF) \quad (3.12)$$

$$Q = -\frac{1}{2} C_1(t) A_0 A_1 \sin\varphi \qquad (AfterLPF) \quad (3.13)$$

The A_0, A_1 and $\cos\varphi$ are constants for a given backscattered signal, so the power spectrum of the signal resembles that of the rectangular signal $C_1(t)$ as shown in Fig. 3.5. The phase shift φ between the LO and backscattered signal can still be obtained from Equation(3.5).

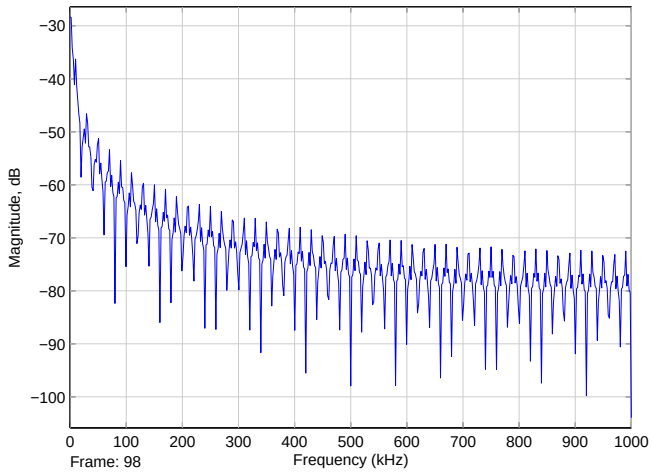

Figure 3.5. Power spectrum of the ASK signal

3.4.2 PSK

As for ASK, there are also two operating modes for PSK as shown in the Fig.3.6. In Fig.3.6 (a), a capacitive reactance is in parallel with the resistive load of the IC, making the total impedance of the circuit capacitive. In Fig.3.6 (b), an inductive reactance is in parallel with the resistive load of the IC and thereby making the total impedance of the circuit inductive. By switching between the capacitive reactance and the inductive reactance, the phase of backscattered signal can be alternated and the bit information can be modulated on the backscattered signal.

With PSK modulation, we can denote the backscattered signal as $A_1 \cos(\omega t - \varphi - C_2(t))$. For the simplicity's sake, we take the binary phase shift keying (BPSK) as an example and assume $C_2(t)$ is a rectangular signal whose value shifts between $-\frac{\pi}{2}$ and $\frac{\pi}{2}$ randomly as shown in the Fig. 3.7. In this case, the output of the two mixers would be:

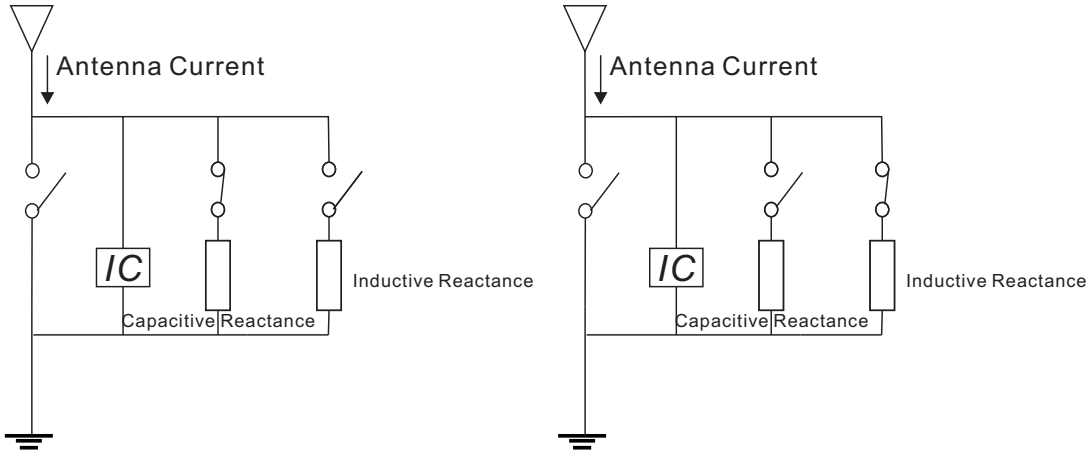

(a) Capacitive (b) Inductive

Figure 3.6. Two operating modes for PSK

$$I = A_0\cos(\omega t) \times A_1\cos(\omega t - \varphi - C_2(t)) = \frac{1}{2}A_1A_0[\cos(2\omega t - \varphi - C_2(t)) + \cos(\varphi + C_2(t))] \tag{3.14}$$

$$Q = A_0\sin(\omega t) \times A_1\cos(\omega t - \varphi - C_2(t)) = \frac{1}{2}A_1A_0[\sin(2\omega t - \varphi - C_2(t)) - \sin(\varphi + C_2(t))] \tag{3.15}$$

After the LPF, the remaining signals would be:

$$I = \frac{1}{2}A_0A_1\cos(\varphi + C_2(t)) \qquad (AfterLPF) \tag{3.16}$$

$$Q = -\frac{1}{2}A_0A_1\sin(\varphi + C_2(t)) \qquad (AfterLPF) \tag{3.17}$$

From Equation(3.16) and Equation(3.17), we can also get the value $\varphi + C_2(t)$ by using Equation(3.5). Since the value of $C_2(t)$ is shifted randomly between $-\frac{\pi}{2}$ and $\frac{\pi}{2}$ and its average value will be 0. Consequently the phase differences φ between the backscattered signal and the transmitted signal can be obtained by averaging the values of $\varphi + C_2(t)$.

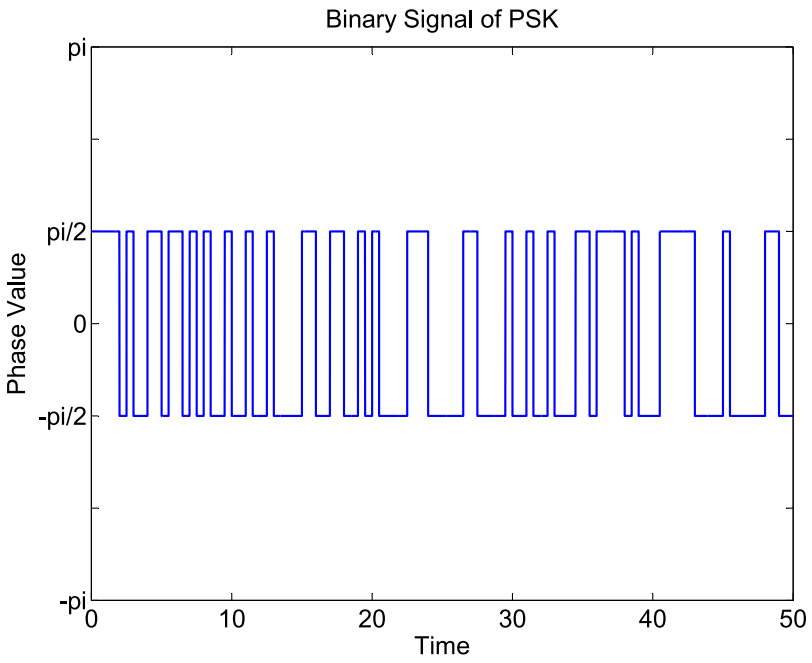

Figure 3.7. Binary signal for PSK

3.5 Signal Leakage from Transmission Chain to Receiver Chain

3.5.1 Two Antenna Configuration

As mentioned in the Chapter 2, the passive RFID reader works in a full duplex mode. When receiving signals, it transmits a CW signal to the tag as well. There are two antenna configurations that can be used to support the full duplex mode: monostatic and bistatic. As is shown in Fig.3.8 (a), the monostatic antenna configuration uses only one antenna for transmission and receive. The transmitted signals and the received signals are isolated from each other with a circulator. The bistatic configuration, on the other hand, uses two antennas for transmission and receiving respectively.

3.5.2 Leakage of Signals

For the monostatic antenna configuration, the transmitted signals leak into the received chain in two ways. The first way is from reflections of the transmitted signals at the

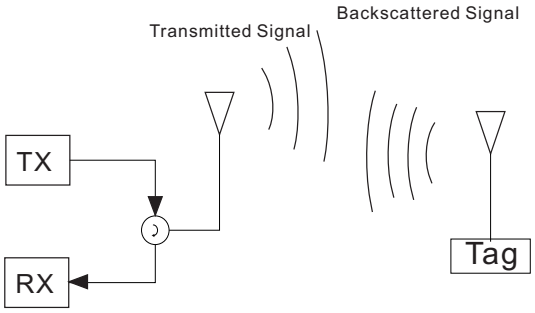

(a) Monostatic

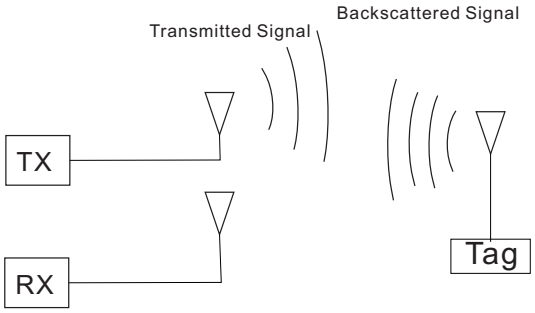

(b) Bistatic

Figure 3.8. Two antenna configurations

antenna due to the mismatch between the transmission chain and the antenna. The other way is through leakage in the circulator itself. The isolation of a typical circulator is about $20dB$. It means that if the transmitter is transmitting a signal of $30dBm$, there is a signal leakage of $30 - 20 = 10dBm$ from the transmission chain into the receiver chain.

The bistatic antenna configuration also has the problem of signal leakage. In this configuration leakage occurs from the coupling between the transmission antenna and the receiver antenna. However, the problem of signal leakage for the bistatic configuration is much less serious than for the monostatic configuration because the isolation between the two antennas can be as high as $40 - 50dB$.

3.5.3 Removal of Leakage Signal

Let the transmitted signal be denoted as $A_0 \cos(\omega t)$, the leakage can be denoted as $A_2 \cos(\omega t - \varphi_{leakage})$. The amplitude A_2 is determined by the amplitude of the transmitted signal A_0 and the isolation between the transmission chain and the receiver

chain. The phase delay of $\varphi_{leakage}$ is caused by the delay from the transmission chain to the receiver chain.

After the two mixers, the leakage signal would be changed into :

$$I = A_0 \cos(\omega t) \times A_2 \cos(\omega t - \varphi_{leakage}) = \frac{1}{2} A_2 A_0 [\cos(2\omega t - \varphi_{leakage}) + \cos(\varphi_{leakage})] \tag{3.18}$$

$$Q = A_0 \sin(\omega t) \times A_2 \cos(\omega t - \varphi_{leakage}) = \frac{1}{2} A_2 A_0 [\sin(2\omega t - \varphi_{leakage}) - \sin(\varphi_{leakage})] \tag{3.19}$$

After the LPF, the remaining signals would be:

$$I = \frac{1}{2} A_0 A_2 \cos(\varphi_{leakage}) \qquad (AfterLPF) \tag{3.20}$$

$$Q = -\frac{1}{2} A_0 A_2 \sin(\varphi_{leakage}) \qquad (AfterLPF) \tag{3.21}$$

In the Equation (3.20) and the Equation (3.21), the values A_0, A_2 and $\varphi_{leakage}$ depend on the system parameters and transmitted signal power. A High Pass Filter (HPF) can be used to mitigate the effect of the leakage signal at baseband and as a result, it will have no effect on the phase measurement. However, if the leakage signal is too strong, it will desensitize the receiver at RF band before it can be filtered out at baseband.

3.5.4 Choice of the Filters

In order to obtain the wanted signal, a bandpass filter (BPF) is required to remove the high frequency signals and the DC leakage signals while passing the wanted signal. For a typical UHF passive RFID system, the unwanted high frequency signals due to the mixing operation that need to be filtered out are at about $1800MHz - 1900MHz$ (twice of the frequency of the CW signals) and the frequencies of the wanted signals

would typically be from $10kHz - 500kHz$ [36] depending on the operating data rate of the RFID tags. Therefore, a BPF with the pass band of $10kHz - 500kHz$ would be effective to filter out the unwanted signals.

3.6 Simulation

In the previous sections, we proposed a structure that can be used to measure the phase differences between the transmitted signals and the backscattered signals. This section describes a software simulation of this proposed structure for ASK modulation. By this software simulation, the effectiveness of this proposed structure is demonstrated.

3.6.1 Simulation Description

Fig. 3.9 shows the proposed structure as implemented in the software Simulink. The module 'LO signal' represents the LO signal and the transmitted signal $\cos(\omega t)$ in the proposed structure. The 'leakage signal' block generates a sinewave of the form $a\cos(\omega t - \varphi_{leakage})$ which has the same frequency as the LO signal but different phase and amplitude. The backscattered signal is generated within the 'backscattered' block which is expanded in Fig. 3.10 and amplitude modulates a random sequence of '2's and 1's onto a sinewave signal with the same frequency as the LO signal but different phase and amplitude. The binary signal is generated by a random Bernoulli binary generator. The sample rate of the simulation is set to be 7.2GHz, allowing a 90^o phase shift for a 900MHz carrier to be implemented by a 2 sample delay. The carrier frequency is assumed to be 900MHz for simplicity and the modulation data rate is set to be 500KHz. After mixing, the resulting signals are filtered by the two LPFs whose frequency response are shown in Fig. 3.11 as well as two HPFs whose frequency response are shown in Fig. 3.12. The filtered signals are processed by a divider and an arctan function module according to Equation (3.5). Several scopes are added to the design to observe the signals.

3.6.2 Analysis of the Results

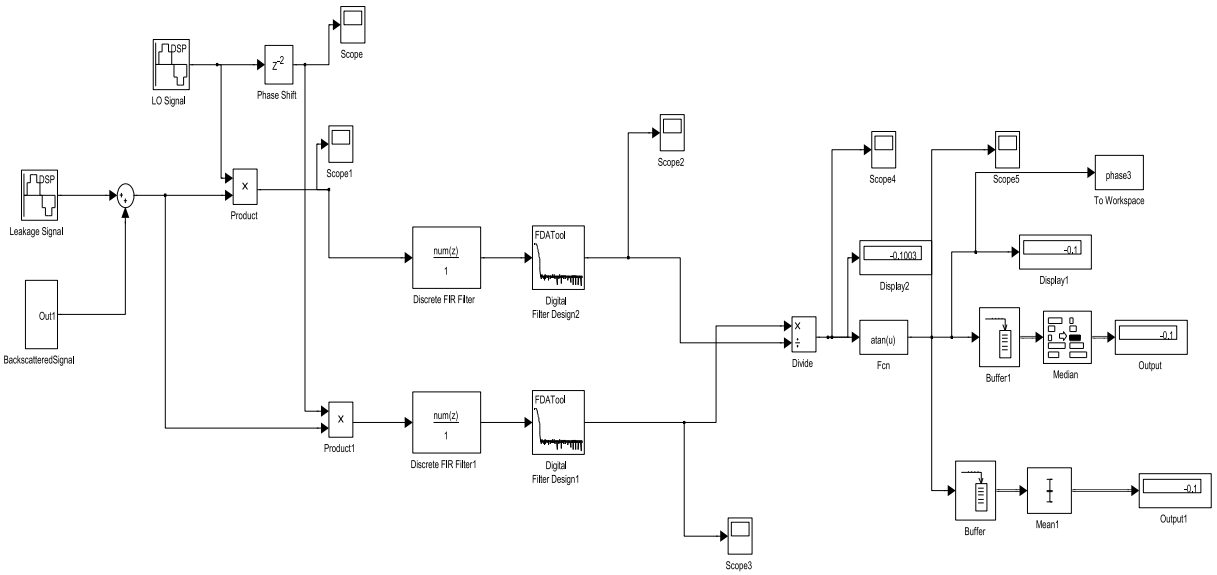

Figure 3.9. Simulation Structure

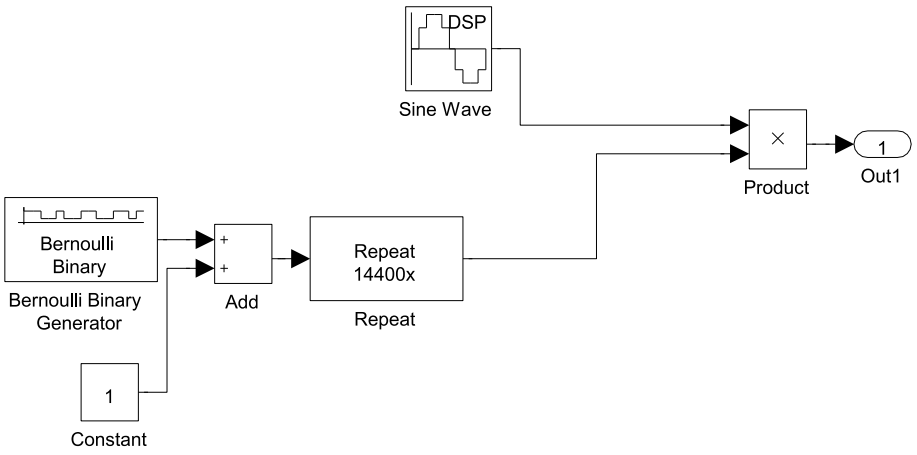

Figure 3.10. Representation of Backscattered Signals

3.6.2.1 Effectiveness of the Structure

The simulation was run eleven times for different preset values of phase difference between the backscattered signal and the transmitted signal (LO signal). The eleven preset phase differences were evenly spaced between $-\frac{\pi}{2}$ to $\frac{\pi}{2}$. After running the simulation, the measured phase differences were compared with the preset values and found to be within 0.001rad of the preset values. From Fig. 3.13, we can see that measured values lie approximately on a straight line when plotted against the true values. Thus the proposed structure measures the relative phase of the backscattered signal reasonably accurately.

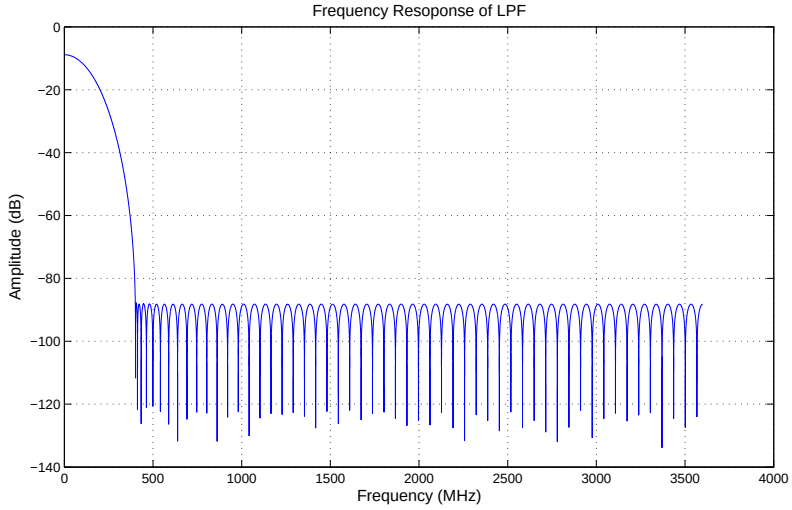

Figure 3.11. Frequency Response of the LPF

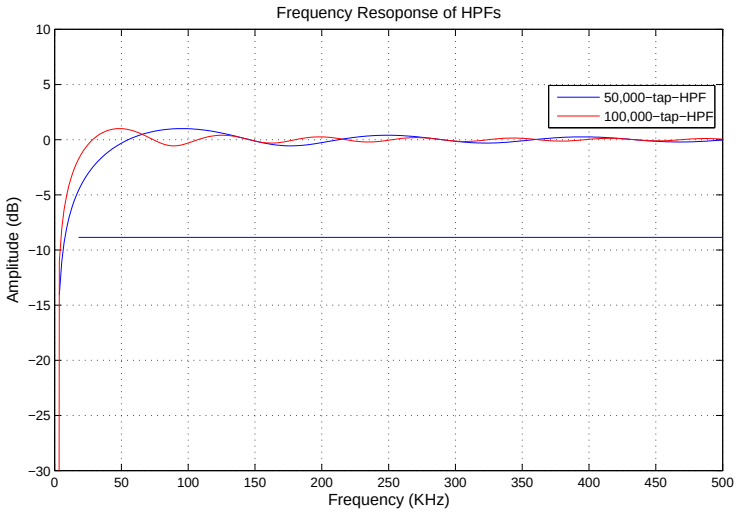

Figure 3.12. Frequency Response of the HPF

3.6.2.2 Impacts of HPFs

During this simulation, two different FIR HPFs were used. Both HPFs have $N+1$ coefficients of the form $[1, -\frac{1}{N}, \ldots\ldots, -\frac{1}{N}]$. The first HPF used $N = 50,000$ taps while the second HPF used $N = 100,000$ taps. These filters simulate analog HPFs implemented using an AC coupling capacitor. The large number of taps are due to the high sampling rate of 7.2GHz used in the simulation which is required to simulate the RF carrier of 900MHz. With any one of these two HPFs, the leakage signal can be canceled completely after the mixer as it has zero amplitude response at zero frequency. However,

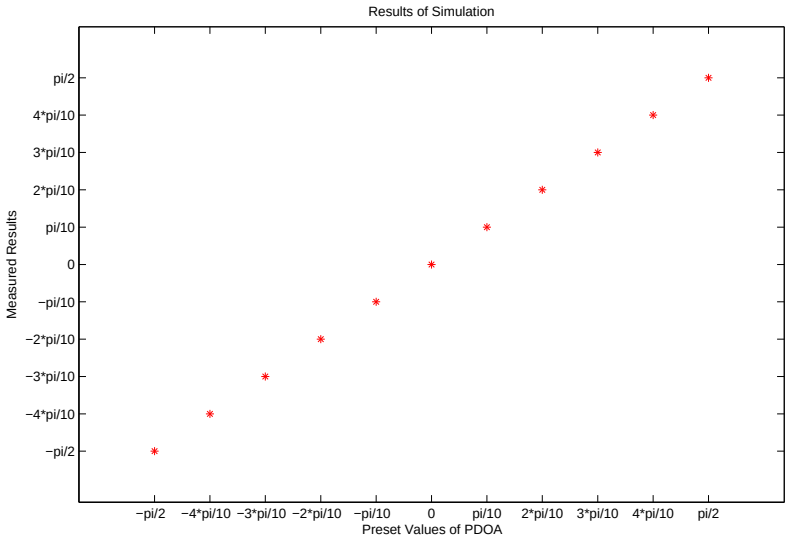

Figure 3.13. The Result of the Simulation

these HPFs will cause distortion to the signal and the measured phase result, especially near data transitions. Fig. 3.14 shows the measured PDOA values with no HPF, a 50,000-tap-HPF and a 100,000-tap-HPF respectively. The true phase shift in this simulation would be -0.1rad. From this figure, we can see clearly that both of the HPFs have small errors in the phase measurement, however, the 50,000-tap-HPF has slightly larger phase errors compared to the 100,000-taps-HPF. This is because the 50,000-tap-HPF cancels more of desired signal than the 100,000-tap-HPF as it has a higher cut-off frequency as shown in Fig. 3.12. It's also notable that the excursion peaks in the phase error occur at the data transitions. However overall the phase errors are less than 0.0002rad and the peaks can be removed by averaging or taking the median over a larger data block.

3.6.2.3 Summary of Simulation

The results shown in Fig. 3.13 indicate the proposed structure is working as expected. Possible error sources are due to:

1. The leakage signal not being completely removed. We have designed the HPF to completely remove the zero frequency signal hence it is completely removed in this simulation. However, this may not be the case in the actual implementation due to nonlinear distortion in the IQ mixers and phase noise.

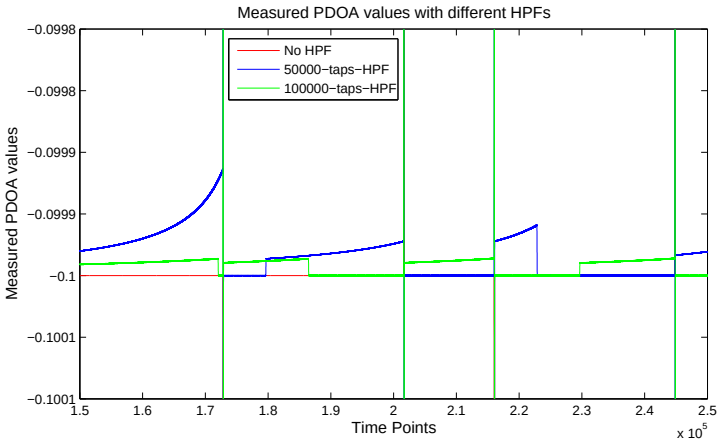

Figure 3.14. Measured PDOA values with different HPFs

2. Incomplete cancelation of the double frequency signal. The LPF has a 100dB attenuation at 1.8GHz so this is negligible in the simulation.

3. Cancelation of the desired signal. If the HPF removes too much of the signal bandwidth, the desired signal will be attenuated and distorted and become very small at some time. This was found to introduce very small phase errors as shown in Fig. 3.14. The cut-off frequency of the HPF needs to be low enough to keep these errors to an acceptable level.

4. Additive noise has not been considered in the simulation but will be there in practice and will cause errors especially if the desired signal is attenuated by the HPF.

3.7 Conclusion

In this chapter, a structure that can be used to obtain the phase differences between the transmitted signal and the backscattered signal has been proposed. After that, a software simulation using Simulink has been used to theoretically verify the effectiveness of the proposed structure. The simulation shows the importance of correctly designing the HPF to cancel the leakage signal. In particular it should have a narrow bandwdith to minimise cancelation and distortion of the desired signal.

Chapter 4

Implementation on a USRP based Hardware Platform

THIS chapter is mainly divided into two parts: tests performed and data analysis. In the first part, we introduced the hardware platform which is built according to the structure proposed in Chapter 3. Based on this platform, the PDOA measurement is performed. The second part analyzes measured results of PDOA based tag positioning.

4.1 Introduction

In the Chapter 3, we have proposed an architecture that can be used to measure phase differences between the transmitted signal and the backscattered signal. After that, a software tool Simulink was used to simulate the proposed structure and in this way the effectiveness of this proposed structure has been verified theoretically. Although the software simulation has verified its validity theoretically, a hardware platform is required to practically verify the effectiveness of the proposed structure. In Section 4.2, the hardware platform that was implemented in this project is introduced. Based on this hardware platform, the PDOA measurement has been performed and the measurement configuration is introduced in the Section 4.3. Finally, The measured results are analyzed in Section 4.4.

4.2 Hardware Test Platform

In this section, we mainly introduce the hardware test platform. This hardware test platform is composed of three main parts: an RFID reader, a tag and an anechoic chamber. The RFID reader is used to transmit a CW signal and at the same time, to receive the backscattered signal from the tag. The tag is used to backscatter the impinging CW signal. Because the project aims to verify the effectiveness of the proposed structure to position tags using the PDOA method, an anechoic chamber is required to remove multipath.

4.2.1 RFID Reader

A USRP (Universal Software Radio Peripheral) N210 [41] from the Ettus Research corporation is used as the hardware platform. This USRP includes a Xilinx Spartan 3A-DSP 3400 FPGA, 100 MSPS dual ADC, 400 MSPS dual DAC. It also has Gigabit Ethernet connectivity to a host computer and through this connectivity, the data can be stored and processed in the computer. The USRP is controlled by a SDRu Transmitter module, SDRu Receiver module and other modules in the Simulink library.

The RFX900 daughterboard for the USRP N210 is used in the project as the front end module of this hardware platform. The RFX900 is a high performance software defined transceiver operating in the 900 MHz band. Its typical power output is 200 mW, and its receiver has a noise figure of 8 dB. In this project, it is used to transmit a CW signal and receive the backscattered signal from the tag simultaneously. There are two different ways to set up this experiment. One way is relatively simple and involves no modifications to the RFX900 but simply uses both the transmit and receive chains as intended. The other way is more complex and involves hardware modifications to the RFX900 board. An HP signal generator (ESG-3000A) and two power amplifiers are used to replace the transmitter module of the RFX900.

4.2.1.1 First Implementation

Using the RFX900 front end directly for this project is rather simple. It just requires plugging the daughterboard into the motherboard and using the software Simulink to control it. Fig. 4.2.1.1 (a) shows the structure proposed in Chapter 3 which we are planning to implement while the Fig. 4.2.1.1 (b) shows how it can be implemented directly on the RFX900 daughtboard. As can be seen in the two figures, the RFX900 has two separate LOs for the downconverting and upconverting respectively. This is not ideal, as both the received and transmit chains should ideally use the same oscillator. Any error in frequency will cause residual modulation on the base-band signal as well as potential problems canceling the leakage signal, which will no longer be at zero frequency. The USRP allows both oscillators to be locked to a pulse per second signal, which means the frequencies should track each other. However, we were not confident about how accurately they could track each other. Also the phase noise on each oscillator would be different as as separate VCOs are used. Hence we decided to modify the daughterboard to used an external LO signal to drive both the transmitter and receiver chain for the second implementation.

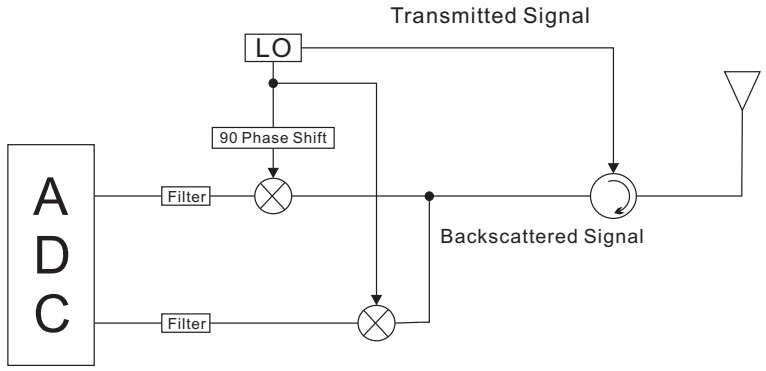

(a) The proposed structure

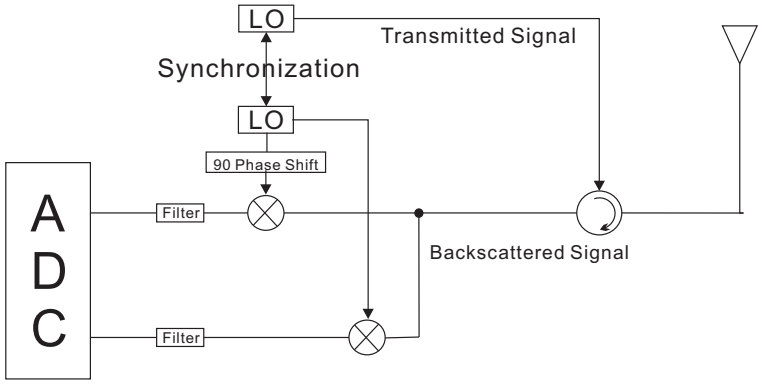

(b) The structure of RFX900

Figure 4.1. Comparison of the proposed structure and RFX900

4.2.1.2 Second Implementation

In the second implementation the USRP is only used as a receiver. It is modified to accept an external LO signal. This LO signal is generated using a ESG 300A signal generator. The transmitter is implemented using two amplifiers and both the transmitter and receiver are connected to the same LO signal derived via a splitter from the signal generator.

Some alterations have been made to the receive chain of the daughterboard RFX900 to allow it to accept an external LO signal. The schematic of the RFX900 is shown in Appendix C, including the changes that were made to incorporate an external LO. Essentially the LO for the down-converting mixer (AD8347) is connected to an external SMA connector, rather than the internal VCO (ADF4360). The structure of the altered daughterboard is shown in the Fig. 4.2 and its photo can be seen in the Fig. 4.3.

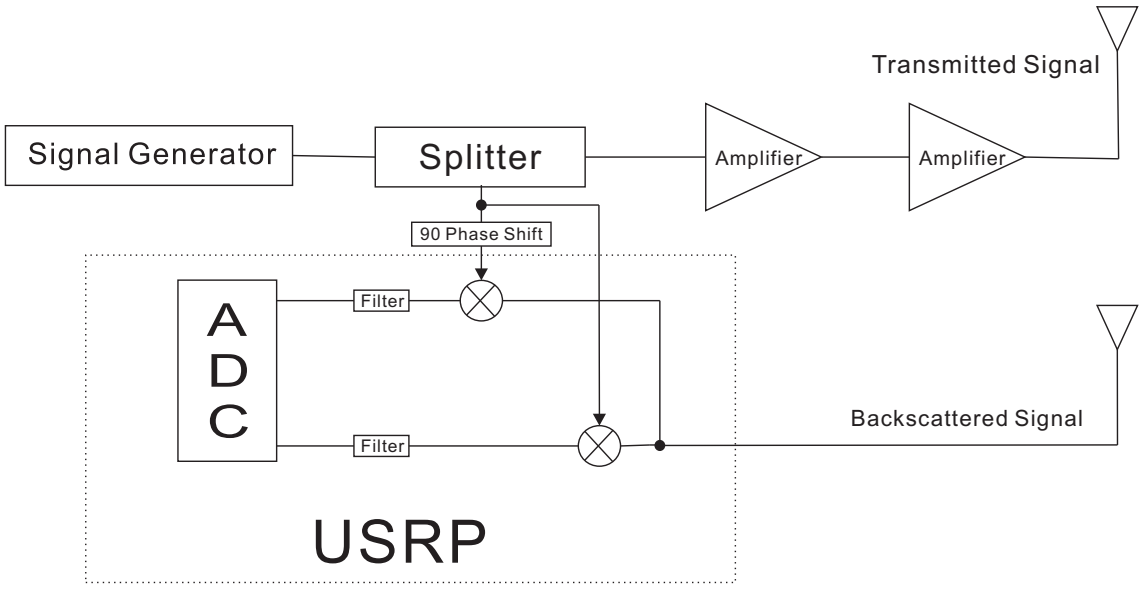

Figure 4.2. The second way to implement the front end

In the project, the bistatic antenna mode is used as seperate antennas are connected to the transmission and the receive chain.

4.2.2 RFID Tag

In this projects, RFID tags designed in the Auto-id Lab of University of Adelaide are used. All of the tags used are passive tags which don't have their own power supply. The read ranges of these tags are more than two meters, although the effective ranges for PDOA based positioning are much shorter.

One of the tags used in this project can be seen in the Fig. 4.4. It is a $7.5cm \times 5.2cm$ tag. These tags were designed according to the EPC Radio-Frequency Identity Protocols Class-1 Generation-2 UHF RFID Protocol for Communications at 860MHz-960MHz [36]. The actual operating frequencies in this project are from the $918MHz$ to $926MHz$ according to regulations from the Australian Communications and Media Authority (ACMA) [42].

When the generated CW signal impinges on the RFID tag, it will be ASK modulated and backscattered to the receive antenna of the RFID reader. The power level of the backscattered signal is at least $6dB$ less than that of the impinging CW signal [43].

Figure 4.3. The altered daughterboard

4.2.3 Test Environment

The PDOA based tag position estimation is expected to be used in an indoor environment. Like other indoor positions techniques, this PDOA based method will be affected by multipath effects. However, the influence of multipath is not considered in this project. In this project, we focus on the verification of the validity of PDOA based positioning methodology without multipath effects. Taking multipath into consideration will be the next step of this research topic in the future.

As shown in the Fig. 4.5, an anechoic box of size of $182cm \times 118cm \times 95cm$ is used for the project in order to remove multipath effects. The inner surface of the anechoic box is covered with special material that can absorb the microwaves substantially. Because most microwave signals that arrive at the inner surface of the anechoic box are absorbed, the level of reflection and refraction is decreased significantly. In this way the multipath effects can be reduced to an acceptable level.

Figure 4.4. The tag used in this project

4.3 Test Configuration

This section introduces how the test is configured. It includes mainly 4 parts. The first part introduces the methodology of this test. The three different methodologies TD-PDOA, FD-PDOA and SD-PDOA introduced in the Section (2.5) are analyzed in this part and finally the FD-PDOA and TD-PDOA are chosen for this project. The second part analyzes the differences between theory and practice mathematically. Methods for system calibration are introduced in this part. After that, the physical test configuration is introduced and a photo of the test configuration is presented. Finally, the operating frequencies are decided and the reasons for this choice are given in the fourth part.

4.3.1 Test Methodology

In Section(2.5), three different applications of PDOA based positioning technique have been introduced: TD-PDOA, FD-PDOA and SD-PDOA. However, only the FD-PDOA is fully investigated in this project. The TD-PDOA application is implemented with some alterations.

Figure 4.5. The test configuration

4.3.1.1 FD-PDOA

As is illustrated in the Section(2.5), the FD-PDOA can be used to estimate the distance between the tag and the reader by measuring phase differences between the transmitted CW signal and the backscattered signal received by the RFID reader. Such a kind of phase difference can the obtained from Equation(3.5). By changing the operating frequency of this RFID system, the calculated phase differences will change as well. By doing the test with a set of different frequencies, we can get a set of different phase differences. Using these phase differences at different frequencies, the distance between the RFID tag and the RFID reader can be obtained by the Equation(2.5)-$d = \frac{c}{4\pi}\frac{\partial\varphi}{\partial f}$. If the calculated distance is the same as the distance measured by a ruler, the validity of the FD-PDOA can be established.

4.3.1.2 TD-PDOA

The TD-PDOA methodology can be utilized to calculate the radial velocity of RFID tags. Unlike the FD-PDOA application, the TD-PDOA positioning system only operates at a fixed frequency. By calculating the phase differences between the transmitted CW signal and the backscattered signal received by the RFID reader at different time points, the radial velocity of RFID tags can be obtained from Equation(2.7)- $V_r = \frac{c}{4\pi * f}\frac{\partial \varphi}{\partial t}$. This project has not directly verified this equation because it would require the tag to move at a fixed radial velocity which is difficult to achieve in our lab. Therefore, we made some alterations to this test procedure.

The test procedure for TD-PDOA is as follows: At time point t_1, calculate the phase differences between the transmitted CW signal and the backscattered signal received by the RFID reader and get the value φ_1. Move the tag to another place and then at the time t_2, calculate the value of phase differences φ_2. Using a ruler to measure the distances d_1 and d_2 between the RFID reader and tag at the two times respectively. In order to verify the validity of the TD-PDOA, we need to satisfy Equation(2.7). we thus need to ensure that:

$$\begin{aligned} V_r &= \frac{c}{4\pi * f}\frac{\partial \varphi}{\partial t} \\ \frac{d_1 - d_2}{t_1 - t_2} &= \frac{c}{4\pi * f}\frac{\varphi_1 - \varphi_2}{t_1 - t_2} \\ d_1 - d_2 &= \frac{c}{4\pi * f} * (\varphi_1 - \varphi_2) \end{aligned} \tag{4.1}$$

From the Equation(4.1), we can see that if the calculated distance differences with $\frac{c}{4\pi * f} * (\varphi_1 - \varphi_2)$ are the same as the measured distance differences $d_1 - d_2$ with a ruler, the validity of TD-PDOA application can be proven. In this way, we don't need to record the time and to make the tag move at a fixed radial velocity.

The validity of TD-PDOA methodology can thus be verified using the following equation:

$$\Delta_d = \frac{c}{4\pi * f} * (\Delta_\varphi) \tag{4.2}$$

4.3.1.3 SD-PDOA

From the Fig.2.5, we can see that SD-PDOA can be used to calculate the direction of the tag. Unlike the other 2 methodologies TD-PDOA and FD-PDOA, this methodology requires building an RFID reader with two or more receive chains. In addition, this methodology is only effective when the distance between the RFID tag and receive antenna is much longer than the distance between the two antennas. Considering the size of the anechoic box, we decided not to experiment with this methodology.

4.3.2 System Calibration

As introduced in the Section(2.5), all these three applications of PDOA based positioning methodology TD-PDOA, FD-PDOA and SD-PDOA are based on an important assumption that the total time t_{total} needed for a signal to be transmitted from an RFID reader and then backscattered by an RFID tag can be written as $t_{forward} + t_{reverse}$. The $t_{forward}$ stands for the time needed for a signal to be transmitted from an RFID reader to a tag while $t_{reverse}$ represents the time required for a signal to be backscattered to the reader. In this way, we get Equation(4.3) as follows:

$$t_{total} = \frac{2d}{c} \tag{4.3}$$

Where d is the distance between the RFID reader and the RFID tag while the c is the velocity of the microwave signal. However, the total time t_{total} doesn't include the $t_{forward} + t_{reverse}$ only. The time for the signal to travel through the cables and other components like amplifiers and filters should also be taken into account. Consequently, the total time can written as:

$$t_{total} = \frac{2d}{c} + \frac{2d_{cable}}{c} + t_{system} \tag{4.4}$$

The $\frac{2d_{cable}}{c}$ factor is the time for the microwave signal to go through the cables. The t_{system} is the delay through by the components like amplifiers and filters.

Form Equation(4.4) and Equation(2.4), we can obtain:

$$\frac{2d}{c} + \frac{2d_{cable}}{c} + t_{system} = \frac{1}{2\pi}\frac{\varphi}{f} \tag{4.5}$$

4.3.2.1 FD-PDOA

From Equation(4.5), Equation(2.8) should be corrected as follows:

$$d = \frac{c}{4\pi}\frac{\varphi}{f} - \frac{c}{2} * t_{system} - d_{cable} \tag{4.6}$$

Since both t_{system} and d_{cable} are constants when the operating frequency is changed, the distance can also be written as:

$$d = \frac{c}{4\pi}\frac{\partial\varphi}{\partial f} - \frac{c}{2} * t_{system} - d_{cable} = \frac{c}{4\pi}\frac{\partial\varphi}{\partial f} - k_0 \tag{4.7}$$

Where k_0 is a constant equivalent to $\frac{c}{2} * t_{system} + d_{cable}$. If we put the tag near the antenna of the RFID reader, we can make the distance to be 0 and in this way, we can obtain the value of k_0 from the following equation:

$$k_0 = \frac{c}{4\pi}\frac{\partial\varphi}{\partial f} \tag{4.8}$$

Once the value of k_0 has been obtained, we can use Equation(4.7) to do the FD-PDOA test.

4.3.2.2 TD-PDOA

Since both the $\frac{c}{2} * t_{system}$ and the d_{cable} can be treated as constants with time, the distance between the RFID reader and the tag can also be written as:

$$d = \frac{c}{4\pi}\frac{\varphi}{f} - k_0 \tag{4.9}$$

Since k_0 is a constant, we can get the radial velocity of the tag as:

$$V_r = \frac{\partial d}{\partial t} = \frac{c}{4\pi * f}\frac{\partial\varphi}{\partial t} \tag{4.10}$$

From the Equation(4.10), we can see that the TD-PDOA application does not depend on the calibration value k_0. Consequently, we don't need to calibrate the system before performing the TD-PDOA test.

4.3.3 Operating Frequencies and Output Power

According to the regulations of ACMA [42], the RFID system can operate in frequencies from $918MHz$ to $920MHz$ with a maximum output power of 1 watts and in frequencies from $920MHz$ to $926MHz$ with a maximum EIRP of 4 watts. In order to simplify this experiment, we make the output power of the RFID reader 1 watt during the whole experiment.

4.3.3.1 FD-PDOA

FD-PDOA based RFID positioning methodology requires phase measurements at serveral different frequencies, we choose 17 frequencies $918MHz$, $918.5MHz$, $919MHz$ ..... $925MHz$, $925.5MHz$, $926MHz$ for the FD-PDOA experiment.

4.3.3.2 TD-PDOA

In the TD-PDOA test, we don't need to change the frequency during the test. Therefore, any frequency in the frequency span $918MHz - 926MHz$ can be used for the TD-PDOA experiment. During the test, the frequency $920MHz$ is chosen as the operating frequency for the TD-PDOA experiment.

4.3.4 Test Setup

As is seen in Fig. 4.6, two patch antennas were used in the anechoic box for transmission and receiving respectively. RF cables are used to connect the antennas to the power amplifier and the USRP. The signal generator is also connected to the power amplifiers and USRP via a splitter. The tag is put on a small paper box at the other end of the anechoic box.

Figure 4.6. The set of the test

4.4 Analysis of Test Results

As is stated in the last section, two applications of the PDOA based positioning TD-PDOA and FD-PDOA are tested in this research project. FD-PDOA has been tested extensively while only limited testing was done on the TD-PDOA scheme.

4.4.1 Two Ways to Implement the Front End Circuit

In Subsection 4.2.1, we introduced two ways to implement the front end circuit of the proposed structure based on the RFX900 daughterboard. One way is to use RFX900 daughterboard which includes both the transmission and the receive chain as introduced in the Section(4.2.1.1). The other approach is to use only the receive chain of the RFX900 as introduced in the Section(4.2.1.2) and use an external signal generator to create a common LO signal for both the transmitter and receiver. This technique requires the RFX900 board to be modified to accept an external LO signal. Using the first method, we found that the measured amplitude of the signals in the I and Q chains was too unstable causing the phase values obtained from the equation $\varphi = \arctan(-\frac{Q}{I})$ to also be unstable. This problem was thought to be due to the lack of a common LO signal for the receive and transmit chains. Therefore, all the useful data was obtained using the second setup in which a signal generator is used to generate a common LO signal used in both the transmit and receive chain.

The reason why the first way of implementing the front end circuit is not effective is that in this way, there are two separate LOs for the transmission chain and the receive chain respectively. Although these two LOs are synchronized with each other using a 1Hz signal, the synchronization rate of 1Hz appears to be not high enough to keep the phase differences between two LOs in an accepted range. As a result, the phase differences between the two LOs may become too large before they are adjusted back and the measured amplitude of signals in the I and Q chains were too unstable. From this test, we can see that, if there are separate LOs in the front end circuit of the PDOA based RFID positioning system, these LOs should be synchronized at a sufficiently high rate.

4.4.2 Data Processing

As stated in the Section 4.2, the USRP based hardware platform is controlled by the software Simulink. The modules in the Fig. 4.7 are used to control the hardware platform to transmit a CW signal and get data from the receive chain. The data obtained

in the I and Q chain are as shown in Fig. 4.8. In Fig. 4.8, the 'SDRu Receiver' block represents the USRP in Simulink. The parameters of this block set up the properties of the USRP data capturing system. For this experiment the USRP was set tup to have a sample rate of 100MHz at each of the I/Q channels. This data are then low-pass filtered and decimated by 32 to $\frac{100}{32}$MHz inside the FPGA. After the decimation, the data are sent accross the ethernet to the PC where it where it comes out of the Data port on the 'SDRu Receiver' block. The data have two channels-real and imaginary which are saved in the matlab workspace through two 'Signal To Workspace' blocks.

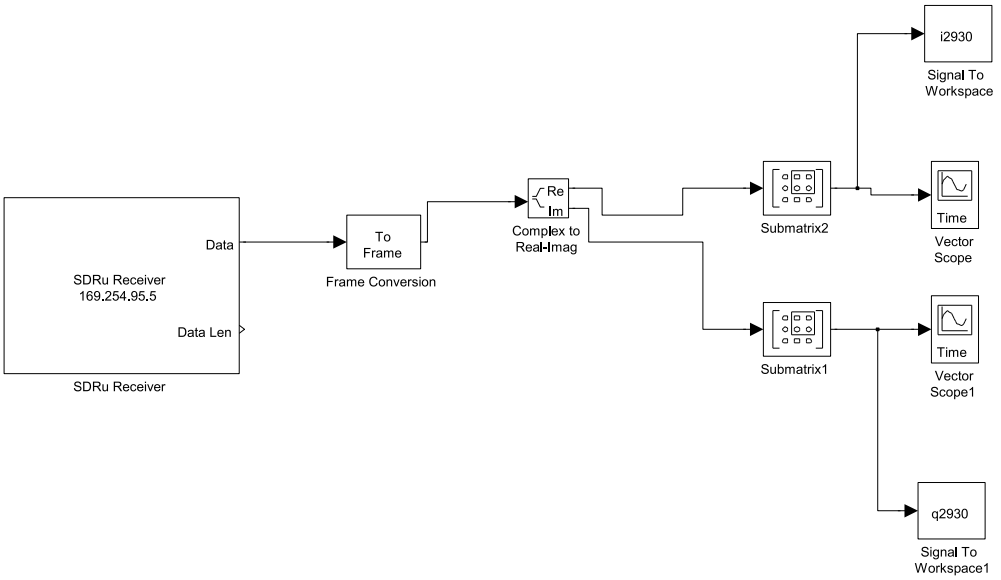

Figure 4.7. Control of USRP

Once we get data from Simulink, we can measure the average amplitude of the I and Q data in the Fig. 4.8 to calculate the phase differences between the transmitted signal and the received signal according to the equation $\varphi = \arctan(-\frac{Q}{I})$. After the phase difference φ_0 has been calculated, more values like φ_1, φ_2 and φ_3 could be obtained in the same way for different operating frequencies (FD-PDOA) or different time (TD-PDOA).

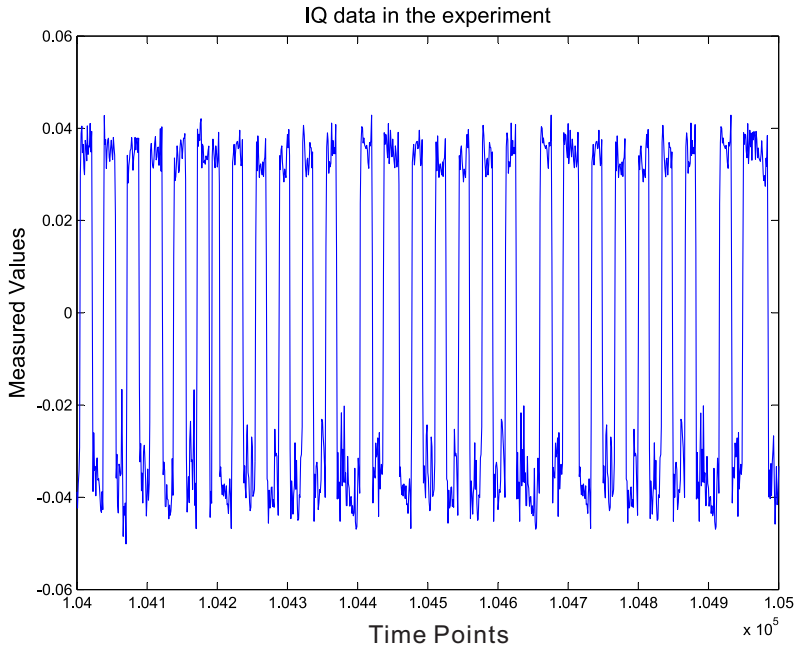

Figure 4.8. I and Q data from the Receive Chain

4.4.3 Results of FD-PDOA

Using the methodology stated in the Subsection(4.4.2), a number of phase differences at different frequencies have been obtained. Using these values, the distance between the RFID reader and the RFID tag can be calculated from the equation $d = \frac{c}{4\pi}\frac{\partial\varphi}{\partial f}$. For example, some FD-PDOA data from different operating frequencies are as shown in Fig. 4.9.

First the system was calibrated by placing the tag directly next to the receive antenna as introduced in Section 4.3.2.1 . The effective distance at this position was 2.969m and corresponds to the cable and component delays in the system. Next the tag was moved to 50cm from the receive antenna. The measured phase differences are shown as a function of frequency in Fig. 4.9 and follow a straight line indicating a pure time delay. Based on the slope at this line, the total delay corresponds to 3.5313m indicating a distance of $3.5313 - 2.969 = 0.5625$m from the receive antenna. The above experiment was repeated for tag positions of $0.7m$, $0.9m$, $1.1m$ and $1.3m$. The test results for the estimated positions are shown in Fig. 4.10.

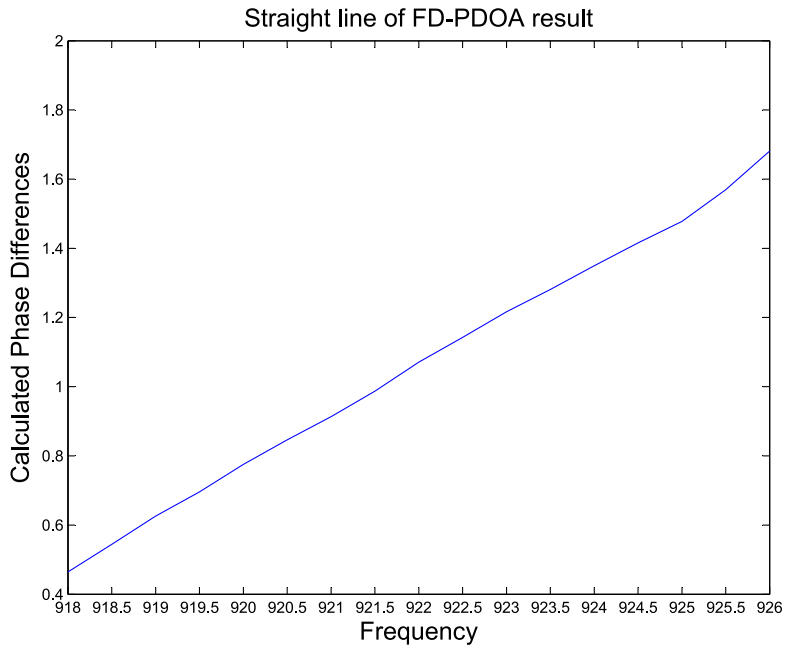

Figure 4.9. Slope of FD-PDOA

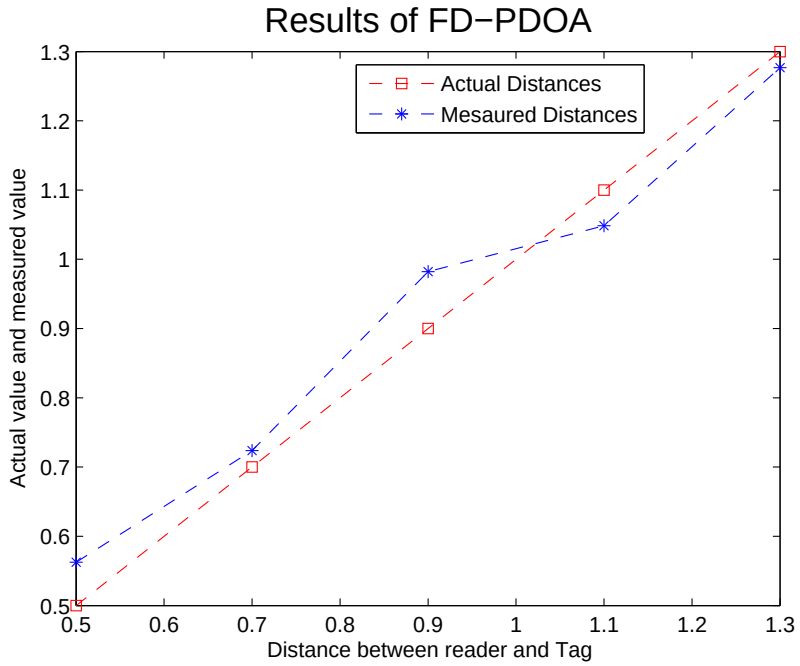

Figure 4.10. The calculated value and the actual value

From the above figure, we can see that the distance values estimated from the phase measurements are similar to the actual distance. Therefore, the hardware platform could be used to calculate the distance between the RFID reader and the RFID tag

through the FD-PDOA methodology. Thus the effectiveness of the proposed structure in this thesis is also verified by this experiment.

4.4.4 Results of TD-PDOA

As is explained in Section 4.3.1.2, the TD-PDOA equation $V_r = \frac{c}{4\pi * f}\frac{\partial \varphi}{\partial t}$ has not been verified directly in this research project. However, we verified the equation $\Delta_d = \frac{c}{4\pi * f} * (\Delta_\varphi)$ instead to prove the effectiveness of the TD-PDOA scheme.

In order to prove the equation $\Delta_d = \frac{c}{4\pi * f} * (\Delta_\varphi)$, we have measured the phase differences between the transmitted signal and the received signal when the tag was placed at different positions at different time points. The tag is placed at positions of $0.7m$, $0.75m$ $0.8m$ $0.85m$ and $0.9m$ away from the RFID reader. After the phase information φ is obtained by the methodology introduced in the Section (4.4.3), these PDOA values are used to calculate the relative radial distance Δ_d with the reference point of $0.7m$. The actual relative distances are $0m$, $0.05m$ $0.1m$ $0.15m$ and $0.2m$ and the measured relative distance are as shown in the Fig. 4.11.

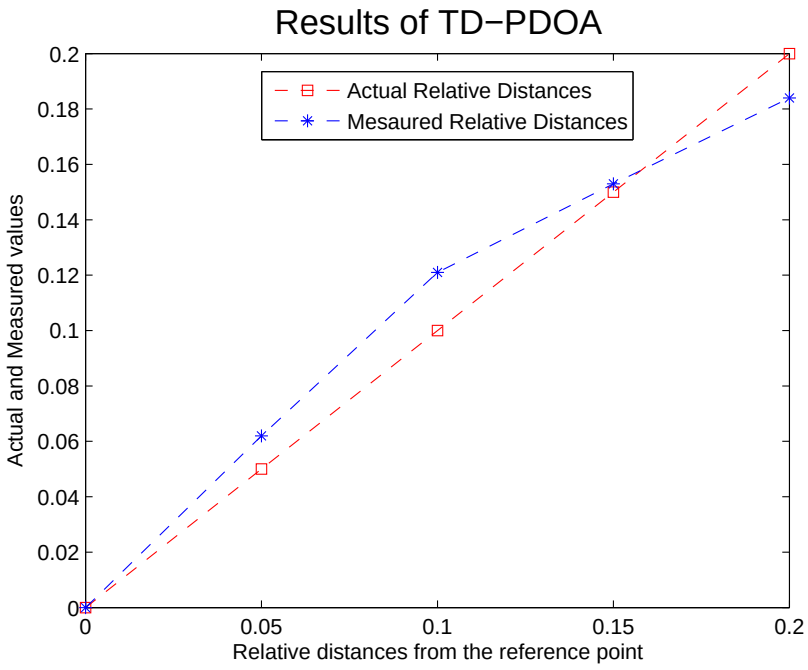

Figure 4.11. Results of TD-PDOA

From the above figure, we can see that the measured relative distance values Δ_d are almost the same as the actual relative radial distance. Therefore, the hardware platform can be utilized to calculate the relative distance Δ_d and if the time differences Δ_t are known, the radial velocity V_r could be calculated from the equation $V_r = \frac{\Delta_d}{\Delta_t}$. Consequently, the TD-PDOA scheme is verified practically in this research project.

4.5 Conclusion

In this chapter, we have introduced the implementation of a hardware platform to verify the PDOA based RFID positioning methodology. The hardware platform is based on the USRP from the Ettus Research corporation and some alterations have been made to the RFX900 daughterboard to accept accept an external LO signal, thus allowing a common LO signal to be used for both transmit and receive. The two schemes FD-PDOA and TD-PDOA have been tested in this research project and the resulting data can be used to prove that the proposed structure can be effectively utilized to obtain PDOA information in passive RFID systems. From the experiment, we can also conclude that if there are two separate LOs for the transmission chain and the receive chain respectively, a very tight degree of synchronization between the two LOs is necessary to estimate position in PDOA based RFID positioning systems.

Chapter 5

Hardware Platform without USRP

THIS chapter introduces a hardware platform without the USRP. This hardware platform is composed of an RF front end board, an ADC board and an FPGA board. With this hardware platform, the FD-PDOA tests have been performed.

5.1 Introduction

In Chapter 4, we have introduced the implementation of a USRP based hardware platform. With this USRP based platform, some experiments have been performed to verify the validity of the proposed structure to get PDOA information. In this chapter, we mainly introduce the implementation of a hardware platform according to the proposed structure without using USRP. This hardware platform is composed of an RF front end board, an ADC board and an FPGA board. Some experiments have also been done to verify the validity of the structure. Developing our own RFID receiver gave us more flexibility in the choice of components, receiver structure and signal processing. It also provides a platform that can be extended to implement a multi channel receiver for SD-PDOA experiments.

5.2 Hardware Test Platform

Like the experiments introduced in Chapter 4, the experiments introduced in this chapter also use an RFID reader, a tag and an anechoic box. The tag and the anechoic box are the same ones as introduced in the Chapter 4. The RFID reader is composed of an RF front end board, an ADC board and an FPGA board as shown in the Fig. 5.1.

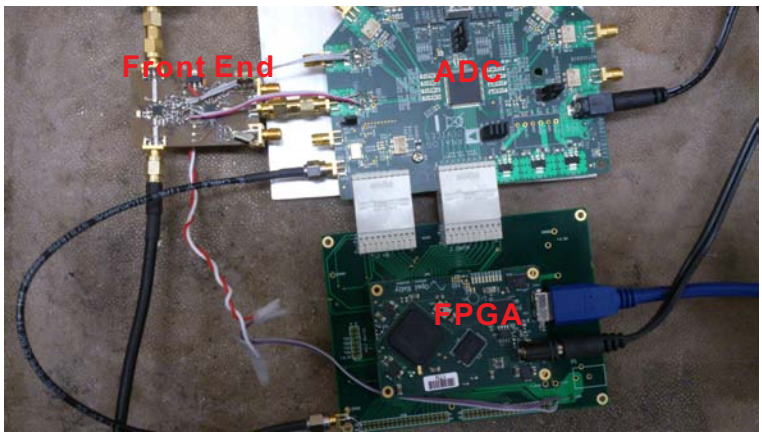

Figure 5.1. Structure of hardware platform

5.2.1 RF Front End board

A block diagram of the RF frount end board is shown in Fig. 5.2. Its main function is to down-convert the RF signal to baseband signal so it can be sampled by an ADC.This RF front end board was designed with the software Altium and the schematic and layout are given in Appendix B. The RF frount end board used the zero-IF architecture and uses the LT5575 I/Q demodulator to convert the RF signal directly to the baseband I and Q channels. Following the mixerchip a filter chip is used to band-limit the signal and amplify it prior to ADC conversion. Unfortunately, the BPF chip was damaged during the soldering work. As a result of that, we connected the output of the mixer chip directly with the input of the ADC board. The anti-aliasing filtering was achieved by changing the values of the capacitors at the output of the mixer chip to implement a single pole low pass filter.

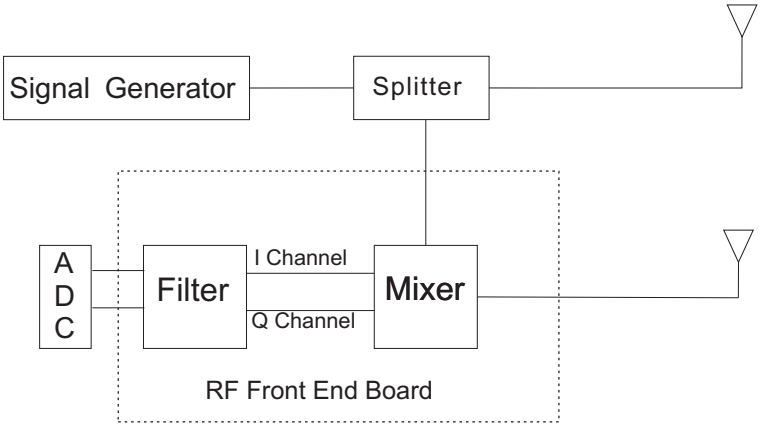

Figure 5.2. Structure of the RF front end board

5.2.2 ADC board and FPGA board

The ADC board is from Analog Devices and in this project, the ADC chip chosen was the AD9271 which includes 8 channel, 12 bit ADC chips each capable of running at up to 50 msps. Each ADC also includes a pre-amplifer with up to 42dB gain. This allows the output of the mixer to be connected directly to the ADC. The ADC board is used to convert the analog signal from the RF front end board into a digital signal that can be processed by the FPGA board. The FPGA board is from Opal Kelly (XEM6310).

In this project, it used simply as an interface between the ADC and PC. It captures a block of data from the ADC into its internal RAM and then sends it to the PC via the USB interface. Both the ADC board and the FPGA board are controlled by a computer through a USB cable.

5.3 Test and Data Analysis

With the hardware platform introduced in this chapter, the FD-PDOA test has been performed. After that, the measured results are analyzed.

5.3.1 FD-PDOA Test

The FD-PDOA test methodology is the same as that introduced in Chapter 4. The same anechoic box and the same RFID tag are also used. The test system has also been calibrated in the same way as introduced in Chapter 4. The measured data were logged on a computer through the USB cable for further processing and analysis.

5.3.2 Data Analysis

The baseband data logged from the system is shown in Fig. 5.3. In this figure, the blue signal shows the received signal in the I channel and the black one shows the signal in the Q channel. The phase of the signal can be calculated from the amplitude ratio of the two signals by using the equation $\varphi = \arctan(-\frac{Q}{I})$.

From a number of measured amplitude ratios of IQ data at different operating frequencies, we can obtain the distance between the RFID reader and the RFID tag with the equation $d = \frac{c}{4\pi}\frac{\partial\varphi}{\partial f}$. By subtracting the calibration factor (as introduced in the Chapter 4), the distance value can be adjusted. In this project, we have got six different distance values $0.5861m$ $0.7414m$ $0.8228m$ $0.9689m$ $1.0301m$ and $1.1299m$ where the actual distance are $0.6m$ $0.7m$ $0.8m$ $0.9m$ $1.0m$ and $1.1m$ respectively. The test results are summarized in the Fig. 5.4.

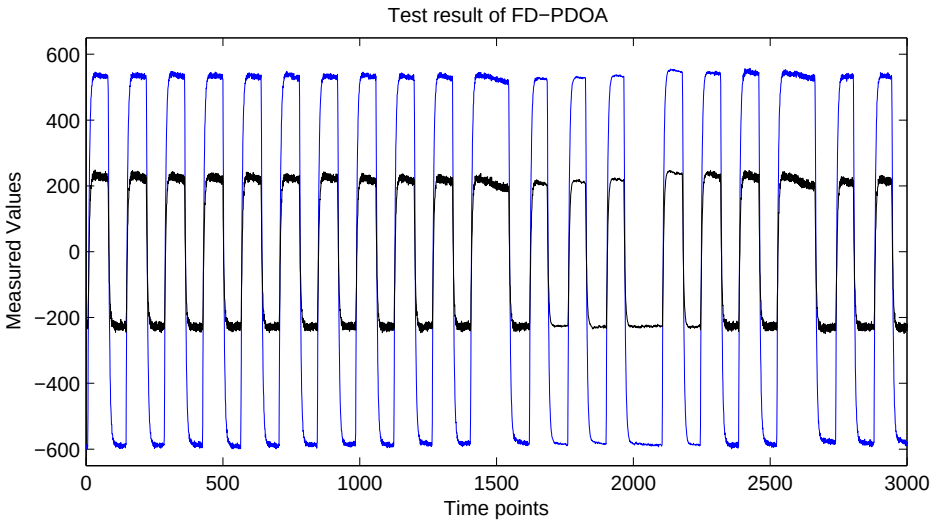

Figure 5.3. Test result of FD-PDOA

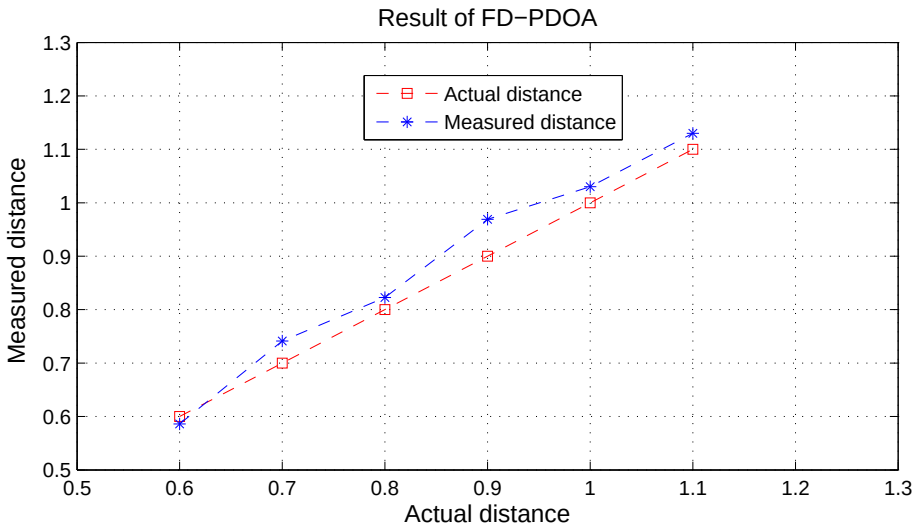

Figure 5.4. Summary of the test

From the above figure, we can see that the calculated distance value are similar to the actual values. That means this hardware platform can be utilized to measure the distance between the RFID reader and the RFID tag.

5.4 Conclusion

In this chapter, we have introduced the second way to build a hardware platform to obtain the PDOA information for indoor positioning application. Through the building

of this platform, we can see that the commercial application of the PDOA based indoor RFID positioning is achievable because the structure of this platform is quite simple and not costly.

Chapter 6

Conclusions and Future Work

THIS chapter concludes the thesis by reviewing the work done, re-summarizing the original contributions, and recommending future work that could be undertaken by others.

6.1 Review of and Conclusions

In Chapter 2, we have stated that the phase differences information between the transmitted signals and the backscattered signals in passive RFID systems could be used for tag positioning. By summarizing and comparing previous academic work, we have concluded some advantages of the phase based passive RFID positioning systems: low cost, long lifespan and small size. However, some disadvantages such as short read range of the phase based passive RFID positioning systems have also been summarized. After that, the three different applications (TD-PDOA, FD-PDOA and SD-PDOA) of the phase based RFID positioning methodology are introduced. The application TD-PDOA can be used to estimate the radial velocity of the tags by comparing the phase differences at different time points. The FD-PDOA scheme is expected to be utilized to calculate the distance between the RFID reader and the tag from the value of phase differences at different operating frequencies. The application SD-PDOA can be utilized to estimate the direction of the tag through the measurement of phase differences of received signals from different receive antennas.

Since the information of phase differences between the transmitted signals and the backscattered signals in passive RFID systems could be used for tag positioning, a methodology is required to obtain the phase differences information in passive RFID systems. In Chapter 3, we have proposed a structure that can be used to obtain the value of phase differences in passive RFID systems. Both the two modulation schemes of the passive RFID systems-ASK and PSK have been considered. After proposing the structure, we stated that a BPF filter can be used to solve the potential problem of leakage signal from the transmission chain to the receiver chain.

To theoretically verify the effectiveness and the efficiency of the proposed structure, a simulation with the software Simulink has been performed. From the simulation, we showed that the proposed structure can be used to measure the phase difference. From the results of this simulation, we also concluded that the higher the amplitude ratio of the leakage signal from the transmission chain to the receiver chain, the worse the performance of the structure.

Software simulation alone is not enough to prove the validity of the proposed structure. Therefore, we have made a hardware platform to practically verify the effectiveness of the proposed structure. This hardware platform is built based on the USRP from the Ettus Research corporation according to the proposed structure. The front end of the hardware platform has been implemented in two ways: firstly using a signal generator as its LO and the secondly using the LO generated on the daughterboard of the RFX900 itself. The results of the experiments on the hardware have shown that the latter way to implement the front end is much worse than the former one because it use two separate LOs for the transmission chain and the receiver chain respectively. With this hardware platform, we have fulfill the FD-PDOA application in full scale and the TD-PDOA to some extent. An anechoic box is used in the experiments to reduce multipath reflections. From the results of these experiments, we can conclude that the proposed structure is practically effective in an indoor environment if multipath effects are small enough.

6.2 Recommendations on Future Work

Due to the limitation of time and equipment, some research problems such as SD-PDOA and multipath effects have not been solved in this research project. All these research problems could be taken as the research gap of other research projects in the future.

6.2.1 Analysis of the Impact of Multipath Effects on PDOA based RFID Positioning Systems

For many indoor positioning techniques, multipath effects are a big problem and the PDOA based RFID positioning methodology is not an exception. In this research project, an anechoic box is used to reduce the impact of the multipath effcts. However, in order to make the PDOA based RFID positioning system applicable in the real indoor environment, the multipath effects are is an inevitable problem and should be

taken into account in the future. Some algorithms should also be proposed to reduce the influence of multipath effects on the PDOA based RFID positioning performance.

6.2.2 SD-PDOA

In Chapter 2, three different applications of the PDOA based RFID positioning methodology are listed: TD-PDOA, FD-PDOA and SD-PDOA. However, the SD-PDOA scheme has not been practically verified with the hardware platform. As is stated in the Section (2.5), more than two receive chains are required to be built in one front end circuit to estimate the direction of the tag. An anechoic chamber is also necessary to do the SD-PDOA experiment in the future.

6.2.3 Cooperative RFID Positioning Systems

In this research project, only one RFID reader is used to estimate the position of the RFID tag. Due to the low read range of a passive RFID reader, only one RFID reader is not enough to cover a normal indoor space. Therefore, multiple RFID readers are needed to cover the indoor space. In addition, if multiple RFID readers can cooperate with each other to estimate the position of the RFID tag, the estimation could be more accurate and reliable. Some techniques such as LANDMARC could be adapted to make multiple RFID readers cooperate with each more efficiently. LANDMARC is a location sensing prototype system that uses Radio Frequency Identification (RFID) technology for locating objects inside buildings [44].

6.3 Conclusion

This chapter summarizes the research carried out in the duration of the master by research study. The research done in this thesis contributes to knowledge of using passive RFID systems to position objects. The thesis provides a general method for (a) the usage of PDOA information to estimate the position of RFID tags, (b) an effective

structure that can be used to obtain PDOA information in RFID systems and (c) implementing a passive RFID system to estimate the position information of RFID tags. The contributions in this thesis could be used by other researchers in their own studies and applications. The work in this thesis and the recommendations on future work in Section 6.2 will create more research possibilities in the field of indoor positioning techniques.

Appendix A

THIS appendix contains a published paper as part of the contributions in this thesis. This paper is accepted for the 2012 International Conference on Computer and Information Science, Safety Engineering which was held in Wuhan, China on June 15-17, 2012.

Yi Li and B. Jamali (2012) Tag position estimation in RFID systems
IN *2012 International Conference on Computer and Information Science, Safety Engineering held in Wuhan, China, June 15-17 2012.*

Appendix B

THIS appendix contains the schematic and PCB layout diagram of the RF front end board.

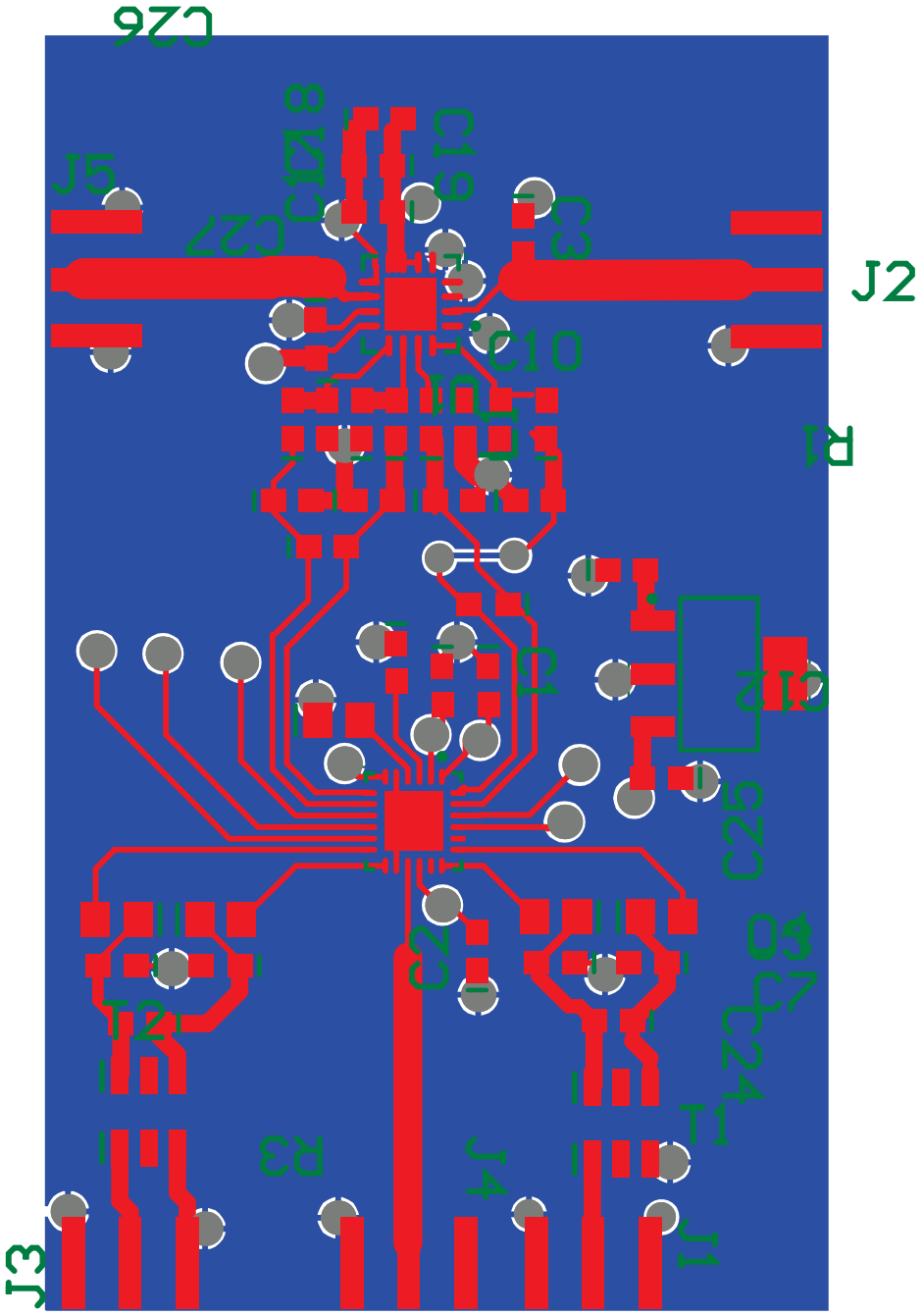

Figure B.1. PCB layout diagram

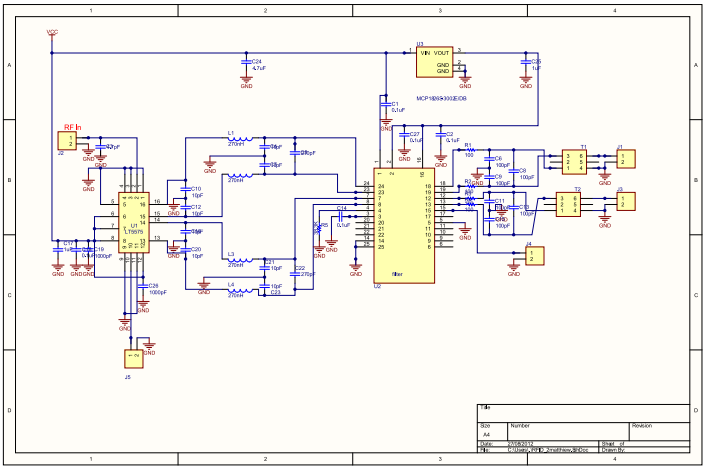

Figure B.2. Schematic diagram

Bill of Materials

<Parameter Title not found>

Source Data From: PCB_Project1.P rjPCB
Project: PCB_Project1.P rjPCB
Variant: None

Creation Date: 27/08/2012 6:17:18 PM
Print Date: 41148 41148.76207

Footprint	Comment	LibRef	Designator	Description	Quantity
0603	Cap	Cap	C1, C2, C3, C4, C5, C6, C7, C8, C9, C10, C11, C12, C13, C14, C15, C16, C17, C18, C19, C20, C21, C22, C23, C24, C25, C26, C27	Capacitor	27
SMA_TOP	SMA	Header 2	J1, J2, J3, J4, J5	Header, 2-Pin	5
0603	Inductor	Inductor	L1, L2, L3, L4	Inductor	4
0805		Res1	R1, R2, R3, R4, R5	Resistor	5
TCM9-1	TCM-9-1	Header 3X2A	T1, T2	Header, 3-Pin, Dual row	2
UF16_L	LT5575	LT5575	U1	Mixer	1
UF24_L	filter	LT6602	U2	filter	1
SOT-223-DB3_L	MCP1826S-3002E/DB	MCP1826S-3002E/DB	U3	1000 mA, Low Voltage, Low Quiescent Current LDO Regulator, 3-Pin SOT-223, Extended Temperature	1
					46

Approved Notes

Figure B.3. Materials used in the project

Appendix C

THIS appendix contains the schematic diagram of RFX900 with modifications.

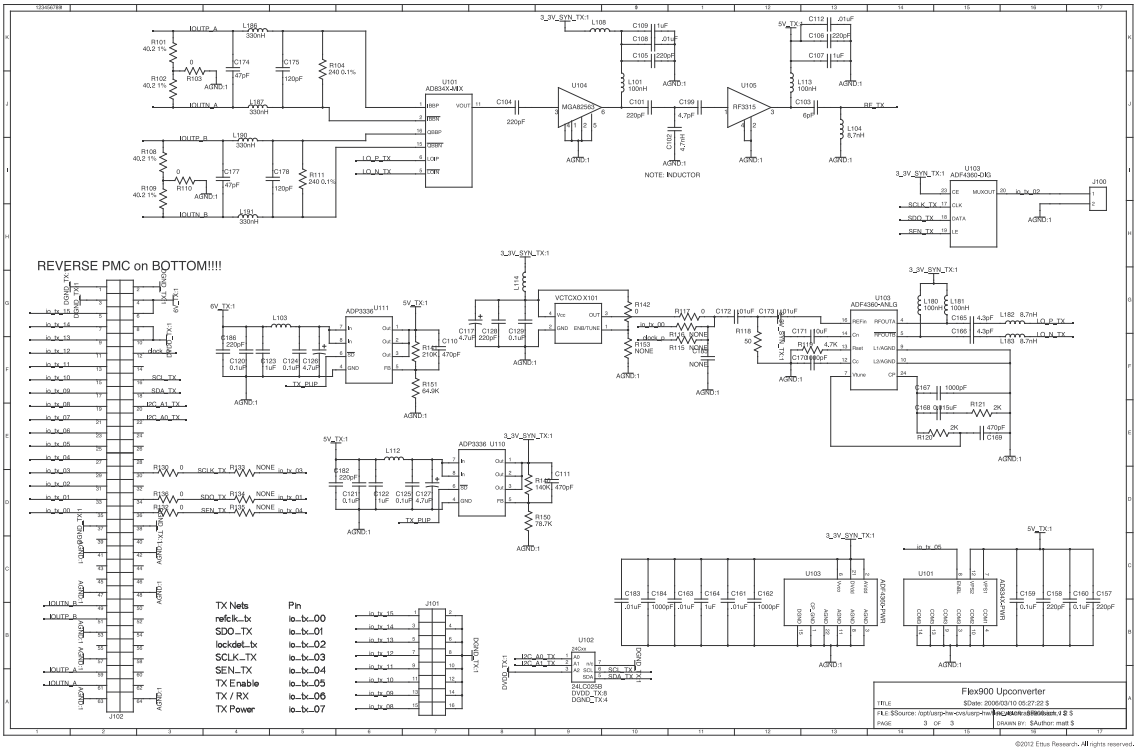

Figure C.1. First page of RFX900

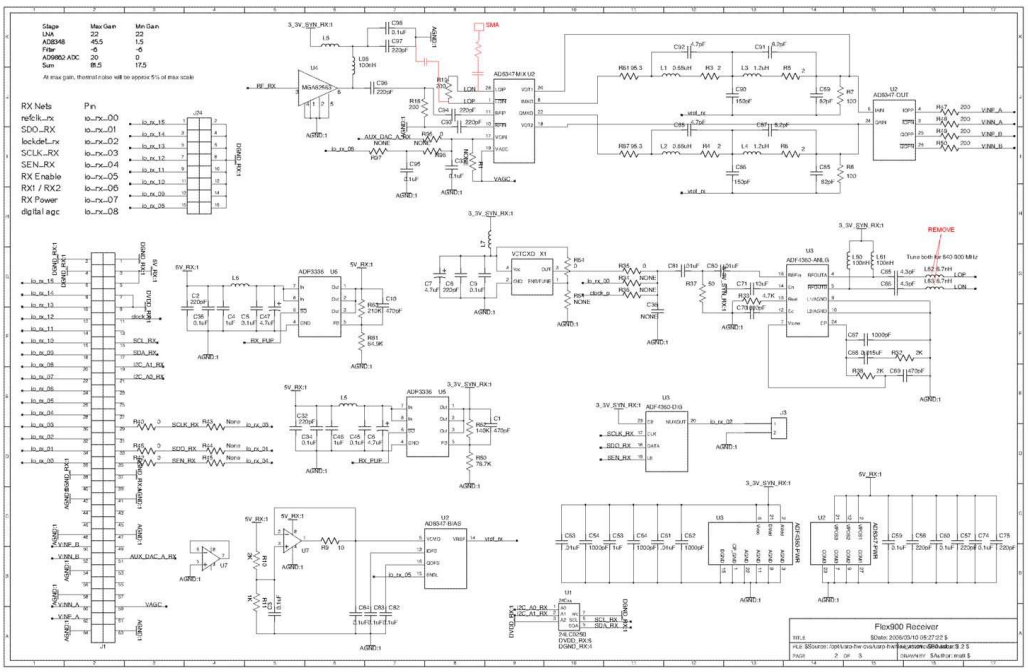

Figure C.2. Second page of RFX900

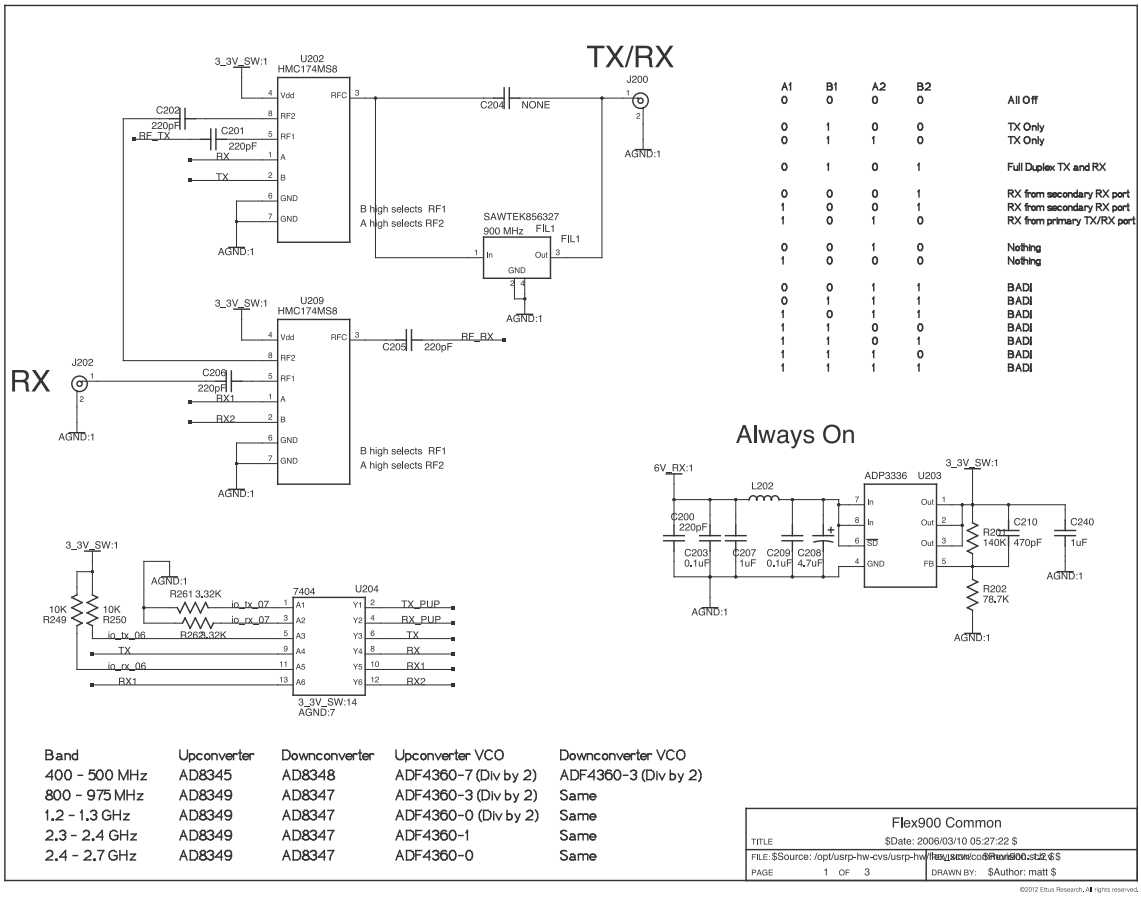

A1	B1	A2	B2	
0	0	0	0	All Off
0	1	0	0	TX Only
0	1	1	0	TX Only
0	1	0	1	Full Duplex TX and RX
0	0	0	1	RX from secondary RX port
1	0	0	1	RX from secondary RX port
1	0	1	0	RX from primary TX/RX port
0	0	1	0	Nothing
1	0	0	0	Nothing
0	0	1	1	BADI
0	1	1	1	BADI
1	0	1	1	BADI
1	1	0	0	BADI
1	1	0	1	BADI
1	1	1	0	BADI
1	1	1	1	BADI

Band	Upconverter	Downconverter	Upconverter VCO	Downconverter VCO
400 - 500 MHz	AD8345	AD8348	ADF4360-7 (Div by 2)	ADF4360-3 (Div by 2)
800 - 975 MHz	AD8349	AD8347	ADF4360-3 (Div by 2)	Same
1.2 - 1.3 GHz	AD8349	AD8347	ADF4360-0 (Div by 2)	Same
2.3 - 2.4 GHz	AD8349	AD8347	ADF4360-1	Same
2.4 - 2.7 GHz	AD8349	AD8347	ADF4360-0	Same

Figure C.3. Third page of RFX900

Bibliography

[1] M. Shell. How to Use the IEEEtran LaTeXClass. [Online]. Available: http://www.ngi2009.eu/IEEEtran_HOWTO.pdf [29 July 2010].

[2] Bureau International des Poids et Mesures. The international system of units (SI). [Online]. Available: http://www.bipm.org/utils/common/pdf/si_brochure_8_en.pdf [29 July 2010].

[3] N. Karmakar, *Handbook of Smart Antennas for RFID Systems*. Wiley-IEEE Press, 2010.

[4] R. Want, "An introduction to rfid technology," *Pervasive Computing, IEEE*, vol. 5, no. 1, pp. 25 – 33, Jan.-March 2006.

[5] D. Sheng, F. Tijun, and H. Weili, "Analysis the impact of the rfid technology on reducing inventory shrinkage," in *Optoelectronics and Image Processing (ICOIP), 2010 International Conference on*, vol. 1, Nov. 2010, pp. 267 –270.

[6] L. Catarinucci, R. Colella, and L. Tarricone, "Integration of rfid and sensors for remote healthcare," in *Applied Sciences in Biomedical and Communication Technologies (ISABEL), 2010 3rd International Symposium on*, Nov. 2010, pp. 1 –5.

[7] Y. Rekik, E. Sahin, and Y. Dallery, "Analysis of the impact of the rfid technology on reducing product misplacement errors at retail stores," *International Journal of Production Economics*, vol. 112, no. 1, pp. 264–278, March 2008. [Online]. Available: http://ideas.repec.org/a/eee/proeco/v112y2008i1p264-278.html

[8] X. Li, T. Wang, J. Chen, J. Chen, Z. Qian, J. Pollard, S. Liu, and J. Yu, "Customer service enhancement using passive rfid," in *Communications Technology and Applications, 2009. ICCTA '09. IEEE International Conference on*, Oct. 2009, pp. 5 –9.

[9] T.-H. Tan and C.-S. Chang, "Development and evaluation of an rfid-based e-restaurant system for customer-centric service," *Expert Syst. Appl.*, vol. 37, no. 9, pp. 6482–6492, Sept 2010. [Online]. Available: http://dx.doi.org/10.1016/j.eswa.2010.02.137

[10] E. Ngai, F. Suk, and S. Lo, "Development of an rfid-based sushi management system," *International Journal of Production Economics*, vol. 112, no. 2, pp. 630–645, April 2008. [Online]. Available: http://www.sciencedirect.com/science/article/pii/S0925527307002010

[11] R. Hornby, "Rfid solutions for the express parcel and airline baggage industry," in *RFID Technology (Ref. No. 1999/123), IEE Colloquium on*, 1999, pp. 2/1 –2/5.

[12] F. Liu, Y. Zou, and W. Liao, "Standard system framework of rfid application in logistics," in *Intelligent Information Technology Application, 2009. IITA 2009. Third International Symposium on*, vol. 3, Nov. 2009, pp. 44 –47.

[13] Y. Huang and G. Li, "Descriptive models for internet of things," in *Intelligent Control and Information Processing (ICICIP), 2010 International Conference on*, Aug. 2010, pp. 483 –486.

[14] "Introduction," in *Principles of Sonar Performance Modelling*, ser. Springer Praxis Books. Springer Berlin Heidelberg, 2010, pp. 3–26. [Online]. Available: http://dx.doi.org/10.1007/978-3-540-87662-5_1

[15] J. Browne, "Celebrating radar technology," *Microwaves and RF*, vol. 50, no. 6, p. 2, 2011.

[16] J. Park, H. Cho, S. Kim, D. Park, A. Kim, and J. Park, "An adaptive parameter estimation method for wireless localization using rssi measurements," in *Future Information Technology*, ser. Communications in Computer and Information Science, J. Park, L. Yang, and C. Lee, Eds. Springer Berlin Heidelberg, 2011, vol. 185, pp. 238–244. [Online]. Available: http://dx.doi.org/10.1007/978-3-642-22309-9_29

[17] Y. Arai and M. Sekiai, "Absolute position measurement system for mobile robot based on incident angle detection of infrared light," in *Intelligent Robots and Systems, 2003. (IROS 2003). Proceedings. 2003 IEEE/RSJ International Conference on*, vol. 1, Oct. 2003, pp. 986 – 991 vol.1.

[18] H. Nonaka and T. Da-te, "Ultrasonic position measurement and its applications to human interface," in *Instrumentation and Measurement Technology Conference, 1994. IMTC/94. Conference Proceedings. 10th Anniversary. Advanced Technologies in I amp; M., 1994 IEEE*, May 1994, pp. 753 –756 vol.2.

[19] K. Yamano, "Self-localization of Mobile Robots with RFID system by using Support Vector Machine," in *Proc. IEEE int. Conf. intelligent robotics and system*.

[20] D. Kim, J. Ha, P. Kim, and K. You, "Tdoa/aoa localization in rfid system using dual indirect kalman filter," in *System Integration (SII), 2011 IEEE/SICE International Symposium on*, Dec 2011, pp. 440 –445.

[21] W. Cully, S. Cotton, and W. Scanlon, "Empirical performance of rssi-based monte carlo localisation for active rfid patient tracking systems," *International Journal of Wireless Information Networks*, vol. 19, pp. 173–184, 2012. [Online]. Available: http://dx.doi.org/10.1007/s10776-012-0189-x

[22] C. Hekimian-Williams, B. Grant, X. Liu, Z. Zhang, and P. Kumar, "Accurate localization of rfid tags using phase difference," in *RFID, 2010 IEEE International Conference on*, Apr 2010, pp. 89 –96.

[23] P. Nikitin, R. Martinez, S. Ramamurthy, H. Leland, G. Spiess, and K. Rao, "Phase based spatial identification of uhf rfid tags," in *RFID, 2010 IEEE International Conference on*, Apr 2010, pp. 102 –109.

[24] E. Kaplan and C. Hegarty, *Understanding GPS: Principles and Applications*, 2nd ed. Artech House, 2005.

[25] B. Peterson, D. Bruckner, and S. Heye, "Measuring gps signals indoors," in *Proceedings of the 10th International Technical Meeting of the Satellite Division of The Institute of Navigation(ION GPS 1997)*, Sept 1997, pp. 615–624.

[26] A. Cleveland, D. Wolfe, M. Parsons, B. Remondi, K. Ferguson, and M. Albright, "Next generation differential gps architecture," in *Proceedings of the 18th International Technical Meeting of the Satellite Division of The Institute of Navigation (ION GNSS 2005)*, Sept 2005, pp. 816–826.

[27] M. Wing, "Consumer-grade global positioning system (gps) accuracy and reliability," *Journal of forestry*, vol. 103, pp. 169–173, 2005.

[28] W. He, E. Tan, E. Lee, and T. Li, "A solution for integrated track and trace in supply chain based on rfid and gps," in *Emerging Technologies Factory Automation, 2009. ETFA 2009. IEEE Conference on*, Sept. 2009, pp. 1 –6.

[29] K. Ozsoy, A. Bozkurt, and I. Tekin, "2d indoor positioning system using gps signals," in *Indoor Positioning and Indoor Navigation (IPIN), 2010 International Conference on*, Sept. 2010, pp. 1 –6.

[30] J. Smith and J. Abel, "The spherical interpolation method of source localization," *Oceanic Engineering, IEEE Journal of*, vol. 12, no. 1, pp. 246 – 252, Jan 1987.

[31] Z. Riaz, D. Edwards, and A. Thorpe, "Sightsafety: A hybrid information and communication technology system for reducing vehicle/pedestrian collisions," *Automation in Construction*, vol. 15, no. 6, pp. 719–728, 2006, cited By (since 1996) 21.

[32] L. Ni, D. Zhang, and M. Souryal, "Rfid-based localization and tracking technologies," *Wireless Communications, IEEE*, vol. 18, no. 2, pp. 45 –51, Apr 2011.

[33] H. Liu, H. Darabi, P. Banerjee, and J. Liu, "Survey of wireless indoor positioning techniques and systems," *Systems, Man, and Cybernetics, Part C: Applications and Reviews, IEEE Transactions on*, vol. 37, no. 6, pp. 1067 –1080, Nov. 2007.

[34] J. Hightower and G. Borriello, "Location systems for ubiquitous computing," *Computer*, vol. 34, no. 8, pp. 57 –66, Aug 2001.

[35] F. Manzoor and K. Menzel, "Indoor localisation for complex building designs using passive rfid technology," in *General Assembly and Scientific Symposium, 2011 XXXth URSI*, Aug 2011, pp. 1 –4.

[36] Radio-Frequency Identity Protocols Class-1 Generation-2 UHF RFID Protocol for Communications at 860MHz-960MHz Version 1.2.0. EPCglobal. [Online]. Available: http://www.epcglobalinc.org/standards/uhfc1g2/uhfc1g2_1_2_0-standard-20080511.pdf [29 July 2010].

[37] J. Zhou and J. Shi, "Rfid localization algorithms and applicationsa review," *Journal of Intelligent Manufacturing*, vol. 20, no. 6, pp. 695 –707, Dec 2009.

[38] B. Van Veen and K. Buckley, "Beamforming: a versatile approach to spatial filtering," *ASSP Magazine, IEEE*, vol. 5, no. 2, pp. 4 –24, April 1988.

[39] Y. Zhang, X. Li, and M. G. Amin, "Array processing for rfid tag localization exploiting multi-frequency signals," in *SPIE Symposium on Defense, Security, and Sensing*, Apr. 2009.

[40] D. Dobkin, *The RF in RFID: passive UHF RFID in practice*, 1st ed. Newnes, 2007.

[41] Ettus Research. USRP N210. [Online]. Available: https://www.ettus.com/product/details/UN210-KIT [16 September 2012].

[42] (2009) Australian Radiofrequency Spectrum Plan 2009. Australian Communications and Media Authority. [Online]. Available: http://www.acma.gov.au [January 2009].

[43] P. Nikitin and K. Rao, "Antennas and propagation in uhf rfid systems," in *RFID, 2008 IEEE International Conference on*, Apr 2008, pp. 277 –288.

[44] X. Yinggang, K. JiaoLi, W. ZhiLiang, and Z. Shanshan, "Indoor location technology and its applications base on improved landmarc algorithm," in *Control and Decision Conference (CCDC), 2011 Chinese*, may 2011, pp. 2453 –2458.